NASA CONTRACTOR REPORT

NASA CR-1615

NASA CR-1615
c. 1

TURBULENT MIXING IN THE INITIAL REGION OF HETEROGENEOUS AXISYMMETRIC COAXIAL CONFINED JETS

by Kirti N. Ghia, T. Paul Torda, and Zalman Lavan

Prepared by
ILLINOIS INSTITUTE OF TECHNOLOGY
Chicago, Ill.
for Lewis Research Center

NATIONAL AERONAUTICS AND SPACE ADMINISTRATION • WASHINGTON, D. C. • MAY 1970

1. Report No. NASA CR-1615	2. Government Accession No.	3. Recipient's Catalog No.
4. Title and Subtitle TURBULENT MIXING IN THE INITIAL REGION OF HETEROGENEOUS AXISYMMETRIC COAXIAL CONFINED JETS		5. Report Date May 1970 6. Performing Organization Code
7. Author(s) Kirti N. Ghia, T. Paul Torda, and Zalman Lavan		8. Performing Organization Report No. None
9. Performing Organization Name and Address Illinois Institute of Technology Chicago, Illinois		10. Work Unit No. 11. Contract or Grant No. NGR-14-004-008 13. Type of Report and Period Covered Contractor Report
12. Sponsoring Agency Name and Address National Aeronautics and Space Administration Washington, D.C. 20546		14. Sponsoring Agency Code
15. Supplementary Notes		

16. Abstract Confined turbulent mixing of dissimilar circular jets is studied in the initial region. A binary isothermal system of non-reacting gases is considered. The central jet consists of a low-velocity high-density stream, while the coflowing annular stream is a high-velocity light gas. This system is characteristic of a gas-core nuclear reactor where minimum mixing is desired. The turbulent boundary layer equations are used to describe the confined jet mixing problem and the numerical solution is obtained by an explicit finite difference scheme. Results were obtained for four jet mixing configurations for which experimental data were available. Thus, correlation of the analysis with experiment is provided for a range of velocity ratio U_2/U_1 from 4.9 to 13.8 and density ratio ρ_1/ρ_2 from 1 to 4.2 for a radius ratio $R_1/R = 0.46$. A formulation is presented for the eddy viscosity ϵ_v and the eddy diffusivity ϵ_m that adequately describes the confined turbulent mixing of heterogeneous streams in the initial region. The empirical parameters used in the ϵ_v expression are presented in terms of the mass flux ratio $U_2\rho_2/U_1\rho_1$ and their relation with the corresponding parameter for homogeneous free jet mixing is interpreted. It is shown that for confined heterogeneous mixing, the kinematic eddy viscosity ϵ_v is a function of both space coordinates r and z. However, the dynamic eddy viscosity $\rho\epsilon_v$ is found to be a very weak function of the transverse coordinate, so that $\rho\epsilon_v$ may be considered to vary only with the axial coordinate z.

17. Key Words (Suggested by Author(s)) Jets, Coaxial, Initial region, Turbulent flow, Mixing	18. Distribution Statement Unclassified - unlimited		
19. Security Classif. (of this report) Unclassified	20. Security Classif. (of this page) Unclassified	21. No. of Pages 90	22. Price* $3.00

*For sale by the Clearinghouse for Federal Scientific and Technical Information Springfield, Virginia 22151

FOREWORD

Research related to advanced nuclear rocket propulsion is described herein. This work was performed under NASA Grant NGR-14-004-008 with Mr. Maynard F. Taylor, Nuclear Systems Division, NASA Lewis Research Center, as Project Manager.

TABLE OF CONTENTS

LIST OF ILLUSTRATIONS

NOMENCLATURE

Symbol	Definition
Latin Letter	
A_1, A_1', A_2	Parameters appearing in Equations (33) and (35)
b	Width of the mixing zone
D_{12}	Diffusion coefficient for binary system
k	Empirical constant in Equation (26)
M_i	Molecular weight of component i
ℓ	Characteristic mixing length
m	Subscript in transverse direction for discretized problem
n	Subscript in axial direction for discretized problem
$N_{Re,1}$	Reynolds Number of inner stream based on molecular viscosity, $N_{Re,1} = \frac{2R_1U_1}{\nu_1}$
$N_{Re,2}$	Reynolds Number of outer stream based on molecular viscosity, $N_{Re,2} = \frac{2(R - R_1)U_2}{\nu_2}$
$N_{Sc,t}$	Turbulent Schmidt Number $N_{Sc,t} = \frac{\epsilon_v}{\epsilon_m}$
p	Static pressure
r	Radial coordinate
$r_{1/2}$	Half radius, for velocity, defined as the value of r at which $v_z = \frac{v_{z,max} + v_{z,min}}{2}$
R	Radius of confining pipe

Nomenclature (Cont'd)

R_1	Radius of inner jet tube
U_1	Average axial velocity of inner stream at entrance
U_2	Average axial velocity of outer stream at entrance
v_r	Time average radial velocity
v_r'	The local fluctuating component of the radial velocity
v_z	Time average axial velocity
$v_{z,1}$	Non-dimensional centerline axial velocity
v_z'	The local fluctuating component of the axial velocity
z	Axial coordinate

Greek Letter

Δz	Step size in z-direction
$\Delta\varphi$	Step size in φ-direction
ϵ_v	Eddy viscosity for momentum
ϵ_m	Eddy diffusivity for mass
λ_i	Boundary values at z = 0, as defined in Equations (6) and (17)
μ	Molecular dynamic viscosity
ν	Molecular kinematic viscosity
π	Constant, = 3.1415297
ρ	Mass average density
σ	Correlating parameter, Equation (32)
φ	Transverse coordinate in φ-z plane
Φ	Value of φ at confining pipe wall
ψ	Stoke's stream function; transverse coordinate in von Mises plane

Nomenclature (Cont'd)

ω_i	Mass fraction of species i
$\omega_{1,w}$	Wall mass fraction

Subscripts

c	Denotes centerline values
r	Denotes radial direction
z	Denotes axial direction
1	Refers to inner stream, i.e. species 1
2	Refers to outer stream, i.e. species 2
i	Species i
max	Maximum value
min	Minimum value
p	Pure component

CHAPTER 1

INTRODUCTION

Confined jet mixing occurs in many devices of practical interest, such as the jet pump or air-to-air ejector, composite propulsion systems as the air augmented rocket, diffusion flames in ducted furnaces, gaseous core reactors for nuclear rocket engines and several fluidic devices. The flow phenomenon in such systems may be laminar or turbulent, depending on the values of the parameters of the system. The parameters of significance in this aspect are the ratios of the initial velocities, densities and radii of the two streams as well as their Reynolds numbers. The laminar case has been analysed in Reference 1; the effect of turbulence in confined jet mixing flows is considered here in the present report.

The present study is directed towards the flow phenomenon occurring in gas-core rocket engines. Therefore, the system considered consists of a central jet of a slow-moving heavy gas and a coflowing annular stream of a fast-moving light gas. Figure 1 illustrates the behavior of such a jet stream in an axisymmetric duct of circular cross-section. Essentially, two idealized regions of flow may be identified.

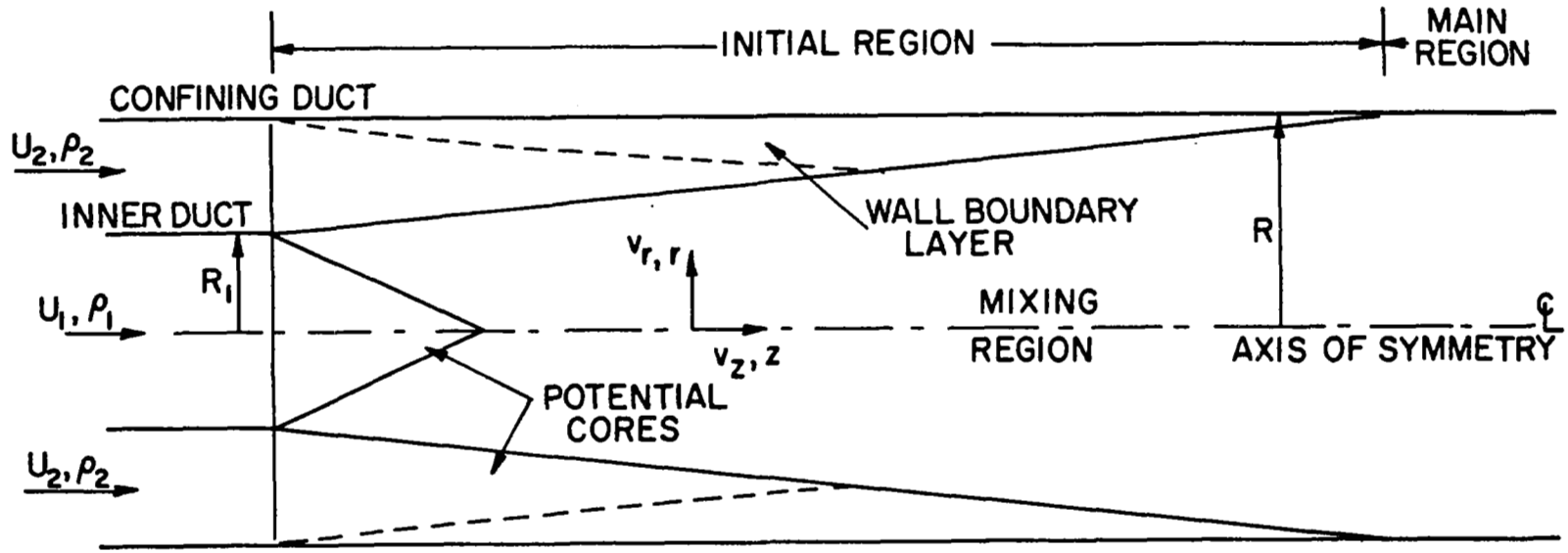

FIGURE 1. CONFINED JET FLOW CONFIGURATION.

The first region extends up to the downstream position where the inner jet fluid mass fraction at the wall first reaches a small prescribed value. This value was chosen arbitrarily as 2% of the entrance mass fraction ω_1 of the inner jet. The flow phenomenon in this region is highly complex. For a short distance downstream of the entrance section, there exists a central core, termed the "potential core," wherein the centerline velocity or the centerline mass fraction or both have undergone no significant depletion.* Separated from this potential zone in the radial direction by a thin shear layer, there also exists a potential zone in the outer stream flow. Large velocity and density gradients prevail in the intermediate shear layer. The thickness of this shear layer increases with distance downstream and quickly erases all of the potential flow zone of the low velocity central jet. The outer potential zone is bounded by the boundary layer at the wall. When the outer stream is faster than the inner, the outer potential zone extends further downstream than the central potential zone. Beyond the end of the outer potential core, the mixing phenomenon is further complicated due to the interaction of the wall boundary layer with the inner jet.

---

* The potential core for velocity may be defined as the region where the axial velocity has changed by less than 0.05 $(U_2 - U_1)$ from its value at the entrance section.

The potential core for mass fraction may be defined as the region where the mass fraction has changed by less than 5% of its value at the entrance section.

Region 1 is often referred to as the initial region. In this initial region, the fast moving stream entrains fluid from the slow moving stream and recirculation phenomena occur if the entrainment capacity of the high velocity stream exceeds the amount of fluid supplied by the low velocity stream. The interest of the present work lies in the initial region for cases where recirculation is absent.

In the second region, mixing and shear flow occupy the entire cross-section of the duct. This region is frequently referred to as the main region.

A survey of the pertinent literature was carried out and is presented in the next section. It will be seen from this survey that turbulent confined mixing has been studied for incompressible as well as compressible cases, but most of the investigations are limited to configurations with the inner jet velocities much greater than the outer stream velocities and the inner jet radius very small as compared to the confining tube radius. For such configurations, the effect of the confining wall is insignificant in the near region and, when recirculation is absent, the flow phenomenon here is similar to the cases of the free jet in a moving secondary stream. On the other hand, in the configurations of present interest, the outer stream is much faster than the central jet and the radius ratio is such as to induce prominent effect due to the presence of the confining wall. Significant density variations are also present. Only the experiments of Leithem, Kulik and Weinstein[2*] come in this category and their recent data are utilized in the present analytical investigation of turbulent confined jet mixing.

* Superscripts denote References.

1.1 Literature Survey

The analyses available for confined turbulent jet mixing involve several simplifying assumptions, and integral techniques are used in general to obtain the solutions. In most of these analyses, the velocity v_z and the shear stress τ were assumed to obey similarity laws, so that expressions for the eddy viscosity ϵ_v and the eddy diffusivity ϵ_m were not needed. In 1955, Craya and Curtet[3] established an approximate theory for confined jet mixing of streams of identical composition. This theory was further developed by Curtet[4,5] and was followed by additional theoretical and experimental studies by Curtet and Ricou[6] and Curtet and Barchilon.[7] The theoretical analysis was based on the assumptions of zero radial pressure gradient, uniform and non-turbulent axial velocity outside the mixing region, and similarity of the axial velocity profiles inside the mixing region. Experimental observations led to the assumption of similar Gaussian velocity profiles in the developing region. Using these assumptions, the governing differential equations were integrated by a momentum integral technique. This approximate analysis resulted in a similitude parameter referred to as the Curtet number C_t^* by Becker et al.[8]

---

* $$C_t = \frac{\left[\frac{R_1}{R}\right]^2 \left[1 + \frac{U_1}{U_2}\right] - \left[\frac{R_1}{R}\right]^2 + 1}{\frac{1}{\sqrt{2}}\left[\left[\frac{R_1}{R}\right]^2 \left[1 + \frac{U_1}{U_2}\right]^2 - \left[\frac{R_1}{R}\right]^4 - 1\right]^{1/2}}$$

This parameter is in fact an expression relating the nozzle and the duct radii and the primary and the secondary flows at inlet, and remains almost constant for the jet mixing flow. This parameter was claimed to play an essential role in the physics of confined jet mixing and it was proposed that if the primary jet were replaced by an idealized point source, then the similitude parameter alone would govern the mixing in the duct. However, this theoretical analysis loses all physical significance in the presence of recirculation which was observed to occur in the initial region of the secondary stream when the outer stream velocity was decreased below a certain low value, keeping the inner stream velocity approximately constant. Further experiments were conducted in order to improve the assumptions made in the approximate theory and thereby extend its applicability to the region downstream of the recirculation eddy in the confined jet mixing flow. These experiments made it possible to characterize the mean structure of the recirculation eddy in terms of the similitude parameter C_t. The assumptions of absence of drag at the confining wall and unidirectional flow in the initial region of the secondary stream were still used, so that the results are yet only approximate.

In 1965, Hill[9,10] carried out analytical studies of an isothermal homogeneous confined jet mixing system in order to predict the mean velocity field in the flow. In this analysis also, an integral technique was used and the shear integrals were evaluated using free jet data. A potential uniform stream was assumed to extend up to the confining wall in the near region where the central jet did not yet reach the wall. This implies that, at the wall, the shear stress and

the boundary layer were assumed negligible, i.e., the effects of a confining wall were not significantly taken into consideration. Approximate self-preservation of the jet flow in the near region was assumed for cases where the jet velocity exceeded that of the outer stream. It was felt that the primary jet potential core could be conceptually replaced by a point source with a virtual origin located approximately in the nozzle exit plane. For cases with recirculation, the static pressure was assumed constant even in the recirculation region, so that the flow external to the inner jet was uniform even when the flow there was reversing. This enabled to retain the relation between the pressure gradient and the velocity gradient in the recirculation region. This approximate analysis led to the formulation of a momentum parameter, referred to later by Exley[11] as the Hill parameter H_p*, which characterized the flow in terms of specified initial conditions. It was pointed out, however, that the assumptions made in the recirculation region were inadequate.

---

* $$H_p = \frac{\frac{U_2}{U_1} + \left[\frac{R_1}{R}\right]^2}{\left[\left[\frac{U_2}{U_1}\right]^2 + 2\left[1 + 2\frac{U_2}{U_1}\right]\left[\frac{R_1}{R}\right]^2\right]^{1/2}}$$

Exley[11] and Becker et al[8] studied confined jet mixing analytically as well as experimentally, but these studies were directed towards investigation of the separation and recirculation phenomena occurring in such flows. Exley carried out a detailed study of the Curtet number and the Hill parameter and suggested that, when the potential core disappears before the jet spreads to the boundary layer at the wall, the Curtet number and the Hill parameter adequately predict the characteristics of the flow in terms of specified inlet conditions. The analysis suggested by Becker et al[8] is similar to that of Curtet and the results are presented in terms of the Curtet parameter. The experimental data of Becker et al showed that the flow pattern of a confined turbulent jet can differ profoundly from that of a free jet, especially in regions of the large recirculation which occurs under the operating conditions of many industrial furnaces.

Dealy[12,13] studied the effects of conditions at the inlet on the flow phenomena in a confined jet mixing system. Dealy concluded that, for systems with low jet-to-confining tube radius ratio, the flow in the near region is indeed independent of the nature of the jet source, has similar velocity profiles and is amenable to analysis by the common momentum integral technique. But for large jet-to-confining tube radius ratios, the mixing mechanism was found to be dependent strongly on the flow conditions in the jet stream. This led to the following useful conclusion regarding Curtet's analysis. In Curtet's analysis, potential flow was assumed to exist near the

turbulent efflux from a long tube. Hence, Curtet's analysis may not effectively predict the characteristics of the flow in confined jet systems with large radius ratios R_1/R for which Dealy's experiments predict dependence of the flow characteristics on the inlet conditions. Further experiments by Dealy also showed that, for fully developed turbulent flow at the jet source, the flow in the near region is primarily a function of the jet Reynolds number. Also, this flow develops more rapidly because of larger turbulent stresses than for the case corresponding to a uniform flow at the jet source.

Trapani[14] carried out an experimental study of turbulent jets with solid boundaries in the transverse direction, in order to investigate their application in certain fluidic devices. Comparison with the flow characteristics of a two-dimensional turbulent free jet showed that the presence of solid transverse boundaries definitely alters the behavior of the flow. The bounded jet (i.e., the jet bounded by plates above and below) was seen to spread less rapidly than the free jet. On the other hand, the confined jet (i.e., the jet enclosed on the top, bottom and the sides) was observed to spread more rapidly than the free jet; this effect was attributed to the development of an adverse axial pressure gradient in the confined jet flow.

One of the few works on confined turbulent mixing with radius ratio R_1/R as large as 0.26 is due to Mikhail[15] who performed experimental as well as theoretical analyses for incompressible

isothermal streams of identical composition. However, even for this radius ratio, the shear stress at the wall was neglected. An integral method was used to analyse the low speed flow in a constant area jet pump. The non-dimensional velocity profiles were assumed to be similar in the entire mixing region and were represented by a cosine function. Experiments confirmed the existence of similarity in the main region (the regions as defined in Fig. 1) and it was concluded that the analysis adequately predicts the gross behavior of the mixing region.

An extensive study of the ducted turbulent mixing process for supersonic flows was carried out by Peters et al.[16,17,18,19] experimentally as well as analytically. The experimental results are presented for a rocket-air mixing system which is typical of the air-augmented rocket. An integral theory for the ducted flow is presented for arbitrary axisymmetric duct geometry and for either frozen or equilibrium chemistry in the mixing zone. The usual boundary layer approximations were assumed to be applicable in the mixing layer which was treated as fully turbulent. At initiation of mixing, the boundary layer was considered negligible as were the viscous effects at the duct wall. Thus, the inviscid portion of the outer stream was one-dimensional and isentropic, while the inviscid portion of the primary jet was also isentropic. The velocity profiles in the turbulent mixing zone were assumed to be similar and were represented by a cosine function. The turbulent shear stress in this variable density mixing layer was treated by

the use of a modified Prandtl eddy viscosity model. The free mixing concept of shear and the velocity profile similarity were assumed to be applicable in the main region also (regions as defined in Fig. 1). The turbulent Prandtl and Lewis numbers of unity were used in the analysis. From the results of analysis and experiment, it was concluded that, while the current knowledge about turbulent flows with chemical reaction is meager, the integral method developed permits reasonably accurate computations of the flow in complex mixing systems such as air-air ejectors and air-augmented rockets.

Emmons[20] also developed an analysis for predicting the flow characteristics in the mixing region of a particle-laden turbulent rocket exhaust and the surrounding air stream (the air-augmented rocket). Neglecting the boundary layer at the confining wall, the turbulent boundary layer equations were used to describe the flow in the mixing system. The eddy viscosity model was assumed to vary with the streamwise coordinate. Finite rate chemistry was considered in the mixing region, although a greatly simplified reaction model was used. The system of partial differential equations governing the flow was transformed using the von Mises transformation and then solved by finite difference methods. The boundary layer equations were also used by Cohen,[21] and Edelman and Fortune[22] in their finite difference analysis of turbulent mixing and combustion of ducted compressible streams.

Leithem, Kulik and Weinstein[2] carried out an experimental investigation of confined turbulent jet mixing for the homogeneous as well as heterogeneous cases. These are the only available experiments with outer stream faster than the inner jet. The flow system consisted of a 3-in. diameter inner stream issuing into a 6-in. diameter confining duct. Air was used for the outer stream while the inner jet consisted of air for the homogeneous case and Freon-12 for the heterogeneous case with density ratio $\rho_1/\rho_2 = 4.2$. The velocity ratio U_2/U_1 ranged from 4.90 to 30.0 for both cases, with absolute values of U_2 varying from 1.5 ft/sec to 40 ft/sec. All data were taken with a constant temperature hot wire anemometer system. The results were presented in the form of radial profiles of density and average axial velocity and radial and axial turbulence intensities for the initial region. It was found that the presence of heavier Freon-12 caused a decrease in the momentum transfer as compared to the homogeneous case, thus leading to preservation of the inner stream for a larger downstream distance. The existence of a concentration potential core was also observed and the length of this pure Freon-12 core was shown to depend on the velocity ratio; the higher the velocity ratio U_2/U_1, the shorter the length of the core.

1.2 Present Study

The literature survey presented shows that the analytical studies available used several simplifying assumptions in order to render the analytical model tractable from the mathematical point of view. Also, the correlation of the analyses is restricted to experimental configurations with very small radius ratio R_1/R when the effects of the confining walls are insignificant, and to cases where the inner stream is much faster than the outer stream. Also, these correlations have been obtained only in the main region, where similarity of the velocity profiles has been assumed. The experimental configurations of Leithem, Kulik and Weinstein[2] belong to the range of present interest and correlations with their recent data are obtained in the present analysis of turbulent confined jet mixing.

The flow problem is formulated as a boundary value problem using the turbulent boundary layer equations. In turbulent mixing problems however, unlike in the corresponding laminar problem, the transport properties of the flow do not depend on the component fluid properties alone, but also on geometric and dynamic factors of the flow system. Therefore, an eddy viscosity model has been formulated in order to correlate the analysis with the data obtained by Leithem, Kulik and Weinstein in the initial region. The equations describing the flow are approximated by their finite difference forms and the solution is obtained by an explicit numerical scheme. Numerical stability is ensured by satisfying Karplus[23] stability

criterion. The finite difference equations are programmed in Fortran IV and solved using the IBM 360/40 computer.

The main contributions of this investigation are:

1. The results provide information about turbulent, incompressible, heterogeneous coaxial confined jet mixing where the presence of the wall may not be neglected. Therefore, the study enables to assess the mixing phenomena in gas-core nuclear reactors.
2. The eddy viscosity model formulated considers both the density variation due to stratification and the confining wall effects in the initial region.

CHAPTER 2

ANALYSIS

2.1 Objective

The turbulent coaxial confined heterogeneous mixing of incompressible jets is studied analytically in the present work. The aims of this investigation are:

1. To obtain the velocity and concentration fields in the initial mixing region of the confined turbulent jet flow.
2. To either modify the existing models or formulate a new model for eddy viscosity in order to take into consideration the effects of stratified flow and confining walls.
3. To correlate the present analysis with the relevant experimental data of Leithem, Kulik and Weinstein.[2]

A phenomenological approach is used for the turbulent flow problem. Therefore, the equations for the mean flow resemble the corresponding laminar flow equations with the molecular transport properties replaced by the eddy diffusivities. The analysis follows along the lines of the laminar analysis of Ref. 1, but will be presented here in brief for the sake of completeness.

2.2 Mathematical Model

The jet mixing problem to be studied is represented mathematically by the boundary layer equations with appropriate boundary conditions. The use of boundary layer equations may be supported by the success with which they have been applied in Ref. 1 in the investigation of laminar confined mixing. Their application to turbulent jet mixing is justified in References 20 and 24 and is also justified in Chapter 4. The present mathematical model is based on the following assumptions:

1. The boundary layer approximations are valid
2. The flow is steady, isothermal and without body forces and chemical reaction
3. Incompressible component fluids

The mathematical model is designed to predict the mixing of two streams as it progresses in the entrance region of a confining pipe of constant cross-section. A typical geometry of the problem is shown in Fig. 1. The solution is obtained by a finite difference method with which any types of entrance velocity profile can be used. The governing equations for the turbulent mixing of two heterogeneous non-reacting streams are well documented [25,26] and are presented next.

2.3 Formulation of Problem in Physical Plane (r,z)

2.3.1 Governing Differential Equations

Continuity Equation

$$\frac{\partial}{\partial r}(\rho r v_r) + \frac{\partial}{\partial z}(\rho r v_z) = 0 \qquad (1)$$

Momentum Equation

$$\rho v_r \frac{\partial v_z}{\partial r} + \rho v_z \frac{\partial v_z}{\partial z} = -\frac{dp}{dz} + \frac{1}{r}\frac{\partial}{\partial r}\left[(\mu + \epsilon_v \rho) r \frac{\partial v_z}{\partial r}\right] \qquad (2)$$

Diffusion Equation

$$\rho v_r \frac{\partial \omega_1}{\partial r} + \rho v_z \frac{\partial \omega_1}{\partial z} = \frac{1}{r}\frac{\partial}{\partial r}\left[(D_{12} + \epsilon_m) r \rho \frac{\partial \omega_1}{\partial r}\right] \qquad (3)$$

Expression for Density

$$\rho = \frac{\dfrac{\omega_1}{M_1}}{\left[\dfrac{\omega_1}{M_1} + \dfrac{\omega_2}{M_2}\right]}\left[\rho_{p,1} - \rho_{p,2}\right] + \rho_{p,2} \qquad (4)$$

The eddy viscosity ϵ_v and eddy diffusivity ϵ_m are unknown in Equations (2) and (3). Their formulation will be discussed in the next chapter.

The pressure gradient dp/dz is calculated using an Equation of Constraint derived on the basis of the momentum equation and on the conservation of mass flow rate across any cross section in the flow region.

Equation of Constraint

$$\frac{dp}{dz} = \frac{1}{\int_0^R \frac{r}{v_z}\,dr} \int_0^R \frac{r}{v_z} \left[\begin{array}{l} v_z^2 \left[\dfrac{\dfrac{\partial \omega_1}{\partial z}}{M_1 M_2 \left[\dfrac{\omega_1}{M_1} + \dfrac{\omega_2}{M_2} \right]^2} \right] \left[\rho_{p,1} - \rho_{p,2} \right] \\ \\ - \rho v_r \dfrac{\partial v_z}{\partial r} + \dfrac{1}{r} \dfrac{\partial}{\partial r} \left[(\mu + \rho \epsilon_v) r \dfrac{\partial v_z}{\partial r} \right] \end{array} \right] dr \qquad (5)$$

2.3.2 Boundary Conditions

1. At the initial section, z = 0

$$v_z(r,0) = \begin{cases} \lambda_1(r) & \text{if } 0 \le r \le R_1 \\ \lambda_2(r) & \text{if } R_1 < r \le R \end{cases}$$

$$v_r(r,0) = 0 \qquad \text{if } 0 \le r \le R \qquad (6)$$

$$\omega_1(r,0) = \begin{cases} \lambda_3(r) & \text{if } 0 \le r \le R_1 \\ \lambda_4(r) & \text{if } R_1 < r \le R \end{cases}$$

2. At the centerline, r = 0

$$v_r(0,z) = \left.\frac{\partial v_z}{\partial r}\right|_{r=0} = \left.\frac{\partial w_1}{\partial r}\right|_{r=0} = 0 \qquad (7)$$

3. At the wall, r = R

$$v_z(R,z) = v_r(R,z) = \left.\frac{\partial w_1}{\partial r}\right|_{r=R} = 0 \qquad (8)$$

Equations (1) through (8), (except for the expressions of eddy viscosity ϵ_v and eddy diffusivity ϵ_m) complete the formulation of the jet mixing problem. The von Mises transformation is used in this analysis in order to facilitate the solution .

2.4 von Mises Transformation

The stream function is defined by

$$\frac{\partial \psi}{\partial r} = \rho v_z r \quad , \qquad \frac{\partial \psi}{\partial z} = -\rho v_r r \qquad (9)$$

and the inverse transformation is given by

$$r^2 = 2\int_0^{\psi} \frac{d\psi}{\rho v_z} \qquad (10)$$

On closer examination, Equation (10) reveals that the number of grid points representing the inner stream decreases as the ratio of the mass fluxes of the outer to the inner streams increases. Hence, to obtain a proper finite difference representation of the inner stream

for these large mass flux ratios without unreasonably increasing the number of steps in ψ-direction, the φ-transformation is used to stretch the ψ-coordinate in the region of the inner stream. The corresponding transformed equations and boundary conditions are presented next.

2.5 Formulation of Problem in φ-Transform Plane (φ, z)

2.5.1 Governing Differential Equations

The φ-transformation is defined by

$$\varphi = \psi^{1/\alpha}$$

$$\text{where} \quad \alpha = \begin{cases} 1 \text{ when } \rho_1 U_1 / \rho_2 U_2 \approx 1 \\ 2 \text{ when } \rho_1 U_1 / \rho_2 U_2 << 1 \end{cases} \tag{11}$$

The equations in the von Mises plane correspond to $\alpha = 1$.

The inverse φ-transformation is defined by

$$r^2 = 2 \int_0^{\varphi} \frac{d\varphi}{\rho v_z \frac{d\varphi}{d\psi}} \tag{12}$$

The Jacobian of this φ-transformation for $\alpha = 2$ is given by

$$J = \frac{\partial(\varphi, z)}{\partial(\psi, z)} = \frac{1}{2\varphi}$$

which is unbounded at $\varphi = 0$. Therefore, particular caution needs to be observed while using the φ-transformation when $\varphi = 0$ which occurs at the duct centerline.

Equations (2), (3) and (5) transform to

$$\frac{\partial v_z}{\partial z} = -\frac{1}{\rho v_z}\frac{dp}{dz} + \frac{d\varphi}{d\psi}\frac{\partial}{\partial\varphi}\left[(\mu + \epsilon_v\rho)r^2\rho v_z \frac{d\varphi}{d\psi}\frac{\partial v_z}{\partial\varphi}\right] \tag{13}$$

$$\frac{\partial \omega_1}{\partial z} = \frac{d\varphi}{d\psi}\frac{\partial}{\partial\varphi}\left[(D_{12} + \epsilon_m)r^2\rho^2 v_z \frac{d\varphi}{d\psi}\frac{\partial \omega_1}{\partial\varphi}\right] \tag{14}$$

$$\frac{dp}{dz} = \frac{1}{\int_o^{\Phi} \frac{d\varphi}{\rho v_z^2 \frac{d\varphi}{d\psi}}} \int_o^{\Phi} \left[\begin{array}{l} -\rho v_r\, r \frac{d\varphi}{d\psi}\frac{\partial}{\partial\varphi}(\rho v_z) \\ + v_z \frac{\partial \omega_1}{\partial z}\left[\frac{\rho_{p,1} - \rho_{p,2}}{M_1 M_2\left[\frac{\omega_1}{M_1} + \frac{\omega_2}{M_2}\right]^2}\right] \\ + \rho \frac{d\varphi}{d\psi}\frac{\partial}{\partial\varphi}\left[(\mu + \epsilon_v\rho)r^2\rho v_z \frac{d\varphi}{d\psi}\frac{\partial v_z}{\partial\varphi}\right] \end{array}\right] \frac{d\varphi}{\rho v_z \frac{d\varphi}{d\psi}} \tag{15}$$

The continuity equation (1) is satisfied identically by the definition of the stream function. For variable density flows, however, the radial velocity v_r can be evaluated from Equation (1) by solving it for $\partial(rv_r)/\partial r$. Thus, the radial velocity appearing

in Equation (15) is evaluated from the equation of continuity in the transformed plane.

$$\frac{d\varphi}{d\psi}\frac{\partial}{\partial\varphi}(r\,v_r) = r\frac{v_r}{v_z}\frac{d\varphi}{d\psi}\frac{\partial v_z}{\partial\varphi} - \frac{1}{\rho v_z}\frac{\partial v_z}{\partial z} - \frac{1}{\rho^2}\frac{\partial\rho}{\partial z} \qquad (16)$$

The expression for density, Equation (4), and the expressions for eddy viscosity ϵ_v and eddy diffusivity ϵ_m formulated in the next chapter remain unaffected by the transformation.

2.5.2 Boundary Conditions

The transformed boundary conditions are

1. At the initial section, z = 0

$$v_z(\varphi,0) = \begin{cases} \lambda_1(\varphi) & \text{if } 0 \le \varphi \le \Phi_1 \\ \lambda_2(\varphi) & \text{if } \Phi_1 < \varphi \le \Phi \end{cases}$$

$$v_r(\varphi,0) = 0 \qquad \text{if } 0 \le \varphi \le \Phi \qquad (17)$$

$$\omega_1(\varphi,0) = \begin{cases} \lambda_3(\varphi) & \text{if } 0 \le \varphi \le \Phi_1 \\ \lambda_4(\varphi) & \text{if } \Phi_1 < \varphi \le \Phi \end{cases}$$

2. At the centerline, $\varphi = 0$

$$v_r(0,z) = \left.\frac{\partial v_z}{\partial \varphi}\right|_{\varphi=0} = \left.\frac{\partial \omega_1}{\partial \varphi}\right|_{\varphi=0} = 0 \qquad (18)$$

3. At the wall, $\varphi = \Phi$

$$v_z(\Phi,z) = v_r(\Phi,z) = \left.\frac{\partial \omega_1}{\partial \varphi}\right|_{\varphi=\Phi} = 0 \qquad (19)$$

2.5.3 Centerline Equations

Since the φ-transformation has an unbounded Jacobian at $\varphi = 0$, suitable limiting processes, together with L'Hospital's rule, are utilized in order to reduce Equations (13) and (14) to the following equations at the centerline $\varphi = 0$.

$$\frac{\partial v_z}{\partial z} = -\frac{1}{\rho v_z}\frac{dp}{dz} + (\mu + \epsilon_v \rho)\frac{\partial^2 v_z}{\partial \varphi^2} \qquad (20)$$

$$\frac{\partial \omega_1}{\partial z} = (D_{12} + \epsilon_m)\rho \frac{\partial^2 \omega_1}{\partial \varphi^2} \qquad (21)$$

Thus the flow problem is represented by Equations (12) through (16) (together with Equations (20) and (21) for the centerline)

and the boundary conditions (17) through (19). The expressions for eddy viscosity ϵ_v and eddy diffusivity ϵ_m have yet to be formulated.

2.6 Method of Solution

A forward marching all-explicit numerical method is used in this analysis. Accordingly, for the transverse derivatives, central differences are used in the interior of the duct and backward differences are used at the duct wall. Forward differences are used for the axial derivatives everywhere except in the continuity equation wherein backward differences are used for the axial derivatives. Substitution of these finite differences in the governing equations leads to linear explicit finite difference equations that are stable under certain conditions. These stability conditions are obtained by using the criterion developed by Karplus.[23] These conditions are only realizable for non-negative axial velocities and are

For momentum equation (13)

1. $\Delta\varphi$ is not limited from stability considerations and is selected from the required resolution and the accuracy of the flow problem.

2. $$\Delta z < \left[\frac{1}{2(\nu + \epsilon_v)} \; \frac{1}{r^2 \rho^2 v_z} \; \frac{1}{\left[\frac{d\varphi}{d\psi}\right]^2} \right]_{m,n} \Delta\varphi^2 \qquad (22)$$

For the diffusion equation (14)

1. There is no restriction on $\Delta\varphi$

2. $$\Delta z < \left[\frac{N_{Sc,t}}{2(\nu + \epsilon_v)} \frac{1}{r^2 \rho^2 v_z} \frac{1}{\left[\frac{d\varphi}{d\psi}\right]^2} \right]_{m,n} \Delta\varphi^2 \qquad (23)$$

Here, m and n denote the transverse and the axial coordinates, respectively.

The stability conditions of Equations (20) and (21) are less stringent than conditions (22) and (23). The more restrictive of conditions (22) and (23)is utilized in the numerical solution. Equations (15), (16), the expression for density, Equation(4) and the expressions for eddy viscosity and eddy diffusivity are unconditionally stable.

The discussion and the development of the turbulent shear model are presented in the next chapter.

CHAPTER 3

DISCUSSION ON EDDY VISCOSITY

3.1 Introduction

In order to obtain a solution of the finite difference equations presented in Chapter 2, it is necessary to establish suitable expressions for the eddy viscosity ε_v and eddy diffusivity ε_m in terms of known quantities. Unfortunately, these turbulent transport coefficients are not fluid properties, as are their laminar counterparts, but they are parameters that depend on the fluid motion, e.g. the level of turbulence, velocity gradient and density gradient. Since turbulent flow is characterized by random fluctuations, the derivation of accurate theoretical expressions for the eddy diffusivities requires a statistical analysis. However, the statistical approach has not proved practical so far,[27] and consequently, one must rely on a semi-empirical approach for determining expressions relating the eddy diffusivities to the flow properties. The derivation of these expressions for the present analysis of confined mixing is based on the results available for unconfined jet mixing. Hence, the relevant turbulent shear models for free jet mixing are first presented. Further detailed discussion on these and other turbulent jet mixing models may be obtained from References 28, 29, 30 and 31.

3.2 Classical Shear Models for Unconfined Jet Mixing

The famous mixing length theory for turbulent shear was formulated by Prandtl in 1925. This theory postulates that the mean value of the fluctuating velocity component in a turbulent flow is equal to the product of the local mean velocity gradient and a characteristic mixing length ℓ. The mixing length is a distance in the flow field such that a fluid element conserves its axial velocity as it moves across this distance. The mixing length ℓ is assumed to be proportional to the local width b of the mixing layer, i.e., $\ell \propto b$. Also, ℓ is assumed to be constant across the mixing layer. Thus, Prandtl's mixing length theory gives the following relation for the turbulent shear stress, or the Reynolds stress, in the axial direction

$$\tau = -\rho \overline{v_z' v_r'} = \rho c^2 b^2 \left| \frac{\partial v_z}{\partial r} \right| \frac{\partial v_z}{\partial r} \tag{24}$$

where c is an empirical constant,

b is the width of the mixing layer,

v_z is the mean axial velocity,

and v_z', v_r' are the local fluctuating components of the axial and the radial velocity, respectively.

Using the concept of eddy viscosity in Equation (24), the expression for the eddy viscosity becomes

$$\epsilon_v = c^2 b^2 \left| \frac{\partial v_z}{\partial r} \right| \tag{25}$$

Thus, Prandtl's mixing length theory yields an eddy viscosity which varies with $\left|\frac{\partial v_z}{\partial r}\right|$ across the mixing layer.

Based on a similar mixing length concept, Taylor derived a vorticity transport theory wherein the vorticity of a fluid element is assumed to be conserved across the mixing length. In Taylor's theory, as well as in Prandtl's, the eddy length scale was assumed to be much smaller than the local width of the mixing layer. However, Taylor's theory has been used much less frequently because of its complexity in all but the simplest flows. It must also be noted that for two-dimensional mixing, the vorticity theory results in the same expression for turbulent shear as obtained from Prandtl's mixing length theory.

In 1942, Prandtl proposed another model for the turbulent eddy viscosity, based on the assumption that the eddy viscosity ϵ_v is related to the local mean velocity gradient across the mixing layer. This formulation implies that the turbulent eddy scale is of the same order as the width of the mixing zone and yields the following expression for the eddy viscosity

$$\epsilon_v = kb(v_{z,max} - v_{z,min}) \tag{26}$$

where k is an empirical constant,

$v_{z,max}$, $v_{z,min}$ are the maximum and the minimum axial velocities respectively, in the mixing layer.

The eddy viscosity is assumed to be constant across the mixing layer, i.e. dependent upon the axial coordinate only. In fact, for an incompressible circular jet exhausting into a quiescent atmosphere, it has been shown that, asymptotically, the width of the jet is linearly proportional to the streamwise coordinate z, whereas the centerline velocity is inversely proportional to z. Therefore, for such a system, Equation (26) yields an eddy viscosity which is constant for the entire flow field.

This model for the eddy viscosity, Equation (26), has been widely applied to a variety of free mixing problems because of its mathematical simplicity and the results it yields agree satisfactorily with experimental data for several flow configurations. It, therefore, forms the basis for most eddy viscosity models existing in the literature, and is used for a particular flow field by appropriately including the effects that may be of significant interest in that case.

3.3 Modifications of Classical Model

For the present problem, it was necessary to account for the following:

1. Effect of a moving external (secondary) stream
2. The case of streams with equal velocities
3. Effect of density difference between the streams
4. Effect of the confining walls

These effects may be considered either individually, by including the corresponding terms in the eddy viscosity expression, or collectively, by suitable modification of the empirical constant k appearing in the ϵ_v model, Equation (26). While no information is available regarding the effect of the confining walls, efforts to include the remaining three effects individually have been made by several investigators and have resulted in various analytical models for the eddy viscosity. However, it cannot be assumed that the eddy viscosity model which is suitable for the present problem will result from a simple superposition of these individual effects. The purpose of the discussion in the remainder of this section is, then, mainly to indicate qualitatively the effects of these additional factors on the formulation of the eddy viscosity model. The final aim, of course, is to formulate an expression for the eddy kinematic viscosity coefficient that can adequately correlate the present analysis with the experimental data of Reference 2 for confined mixing.

3.3.1 Effect of a Moving External Stream

From experiments with unconfined mixing of moving streams of identical composition, Forstall and Shapiro[32] deduced that the presence of a moving secondary stream causes a decrease in the rate of spread of the central jet. Measured in terms of the half radius $r_{1/2}$*, the spreading of the jet was no longer linear with

---

* The half radius $r_{1/2}$ is the radius at which the local axial velocity v_z is equal to $0.5(v_{z,max} + v_{z,min})$.

the downstream distance. In fact, it was shown that, to a good approximation, the growth of the half radius may be given by

$$r_{1/2} \sim z^{1-U_2/U_1} \tag{27}$$

Furthermore, for the centerline velocity decay, it was found that

$$\frac{v_{z,c} - U_2}{U_1 - U_2} \sim \frac{1}{z} \tag{28}$$

Substitution of Equations (27) and (28) into (26) reveals that, for the case of a moving secondary stream, ε_v must depend on the axial coordinate z.

3.3.2 The Case of Streams with Equal Velocities

The various eddy viscosity models available today are the result of attempts by several investigators to include the case of equal stream velocities within the framework of Prandtl's original hypothesis for free turbulent flow. Prandtl's classical model, as given by Equation (26), leads to the obvious realization that $\varepsilon_v = 0$ when $v_{z,max} = v_{z,min}$, so that two streams having equal velocities flow along as segregated, without mixing. This implication has been demonstrated to be incorrect by the results of the experiments of Forstall and Shapiro[32] and Alpinieri.[33] Recognizing this disparity between Prandtl's model and the experimental observations, Ferri et al[34] suggested a new expression for the eddy viscosity

$$(\rho\varepsilon_v)_c = 0.025\, r_{1/2} \left[(\rho v_z)_{max} - (\rho v_z)_{min} \right] \qquad (29)$$

This expression was obtained by extensive correlations of free jet data. It was concluded that the effect of a density difference in the flow field on the form of the eddy viscosity may be accounted for by the inclusion of a density term as in Equation (29). This form for ε_v eliminates the objection to Prandtl's model, Equation (26), when $v_{z,max} = v_{z,min}$, but clearly, it results in a similar difficulty when $(\rho v_z)_{max} = (\rho v_z)_{min}$. Consequently, it shows little value for general application. In order to circumvent such anomalies, Alpinieri[34] considered the eddy viscosity ε_v to be proportional to the sum of the mass flux and the momentum flux, and proposed the following relation for ε_v

$$\frac{(\rho\varepsilon_v)_c}{\rho_1 U_1 R_1} = 0.025\, \frac{r_{1/2}}{R_1} \left[\frac{\rho_2 v_{z,c}}{\rho_1 U_1} + \frac{\rho_2 U_2^2}{\rho_1 U_1^2} \right] \qquad (30)$$

It may be mentioned here that Equations (29) and (30) have been used for extensive correlations but only in the similarity region of a carbon dioxide-air system and a hydrogen-air system with $R_1/R = 0.25$ and U_1/U_2 ranging between 0.47 and 1.25 while $U_2 = 650$ ft/sec. No statement may be made regarding their application to other jet mixing configurations. In fact, this is true for all available expressions for ε_v because of the lack of complete and accurate data used in studying any eddy viscosity model.

Furthermore, the situation that Equations (29) and (30) may both be used to correlate the same experimental data is solved by the results obtained by Ragsdale and Edwards[35] in their analytical and experimental study with an air-bromine system. In their analytical study, various expressions for eddy viscosity were compared on a consistent basis. It was concluded that modifications of Prandtl's hypothesis for turbulent shear flow that introduce mass flux or momentum flux or both, rather than velocities, produce expressions whose differences are more apparent than real. It was shown that these various expressions predict essentially the same eddy viscosity as long as they are applied only within the range of conditions for which they have been experimentally verified. Ragsdale and Edwards explained that this is perhaps because the initial turbulence present in the streams contributes significantly to the coaxial mixing process and may dominate the situation, for nearly equal stream velocities.

3.3.3 Effect of Density Difference between the Two Streams

Density differences may arise within the jet mixing region either due to compressibility effects, as in the case of heated jets and supersonic flows, or due to jets of different composition. Experimental studies of a jet exhausting into a quiescent stream of different density were performed by Corrsin and Uberoi[36] using heated jets and by Keagy and Weller[37] using jets of different composition. In both cases, the asymptotic decay of the centerline

velocity fits a z^{-1} power law reasonably well. Also, the linearity of the half radius $r_{1/2}$ with the axial coordinate z, as observed in constant density mixing, is still valid. However, the rate of linear spread depends strongly on the difference between the densities of the two streams. In fact, a decrease in the jet density with respect to that of the secondary stream causes an increase in the rate of spreading of the jet. Therefore, it is seen that for unconfined mixing, a density difference between the two streams produces no additional axial variation in the eddy viscosity ϵ_v besides a change in the value of the empirical constant in Prandtl's formulation, Equation (26).

The radial variation introduced in the eddy viscosity ϵ_v by a density difference in the mixing streams was accounted for by Ferri et al[34] by using ϵ_v as given by Equation (29). Ting and Libby[38] postulated the following relation between the eddy viscosity for constant density mixing and that for variable density axisymmetric flows

$$\epsilon_v = \epsilon_v^* \left(\frac{\rho_o}{\rho} \right)^2 \frac{1}{r^2} \int_o^r 2 \frac{\rho}{\rho_o} r \, dr \qquad (31)$$

where ϵ_v^* is the eddy viscosity for constant density flows and ρ_o is a reference density.

As seen from Equation (31), the transformation of Ting and Libby is essentially a conversion of the constant density eddy viscosity ϵ_v^* to one applicable for flows with density variations

either due to compressibility or stratification. While this transformation admits possible practical application, no definite form of ϵ_v^* or ρ_o is suggested and the results vary depending on the forms of ϵ_v^* and ρ_o used.

It is seen from the above discussion that several attempts have been made in order to modify Prandtl's classical model for free turbulent shear in order to study variations of the free jet mixing problem. However, not one of them includes all of the effects that are significant in the present problem. The following section discusses the eddy viscosity model used in the present analysis to include the effects listed in Section 3.3.

3.4 Eddy Viscosity Model Proposed for Present Analysis

After suitable redefinition of the constant in Prandtl's classical model, the eddy viscosity expression becomes

$$\epsilon_v = \left[\frac{v_{z,max} + v_{z,min}}{4\sigma^2} \right] z \qquad (32)$$

where σ is a non-dimensional correlating parameter. This form of the eddy viscosity ϵ_v was used by Pai[29] and Bauer[39] for unconfined jet mixing. For an incompressible free jet exhausting into a quiescent atmosphere, σ was found to be twelve.[29] For two dimensional mixing of two moving streams, Korst[40] has proposed the values of σ in terms of velocity ratio of the two streams.

Equation (32) is applicable for the case with a moving secondary stream. Also, this form of the eddy viscosity expression does not display the objection raised for Prandtl's original model for the case of equal stream velocities.

Equation (32) will be used for the eddy viscosity in the present analysis of confined heterogeneous mixing. The two important effects that remain to be included in the proposed model are the effects due to density variation in the streams and the effects of the confining walls. These are jointly accounted for by a suitable radial variation in the parameter σ according to the following considerations.

The region of interest for the present analysis is the initial mixing region. In this region, the value of ϵ_v required near the central axis of the jet should be approximately that for unconfined mixing and the value of σ at the centerline may be estimated from Korst's[40] results for σ. Near the interface of the inner and the outer streams, mixing is enhanced by the large gradients of velocity and density prevailing here. Therefore, the value of the eddy viscosity ϵ_v near the jet interface must be larger than its value at the centerline. Further, at the edge of the mixing zone, the shear decreases to zero, and, in the viscous sublayer at the confining wall, the Reynolds stress is zero and the molecular kinematic viscosity dominates. Thus, the value of ϵ_v should decrease almost to zero at the wall.

These considerations show clearly that, for the present problem, the eddy viscosity must vary radially across the cross-section of the confining pipe. Then, from Equation (32), it follows that the parameter σ also varies with the radial coordinate. The approximate shapes suitable for ε_v and σ are shown in Figures 2a and 2b respectively. This shape of σ may be represented by an expression of the form

$$\sigma = A_1 e^{r/R_1} \cos \pi \frac{r}{R_1} + A_2 \tag{33}$$

where A_1 and A_2 are such that their sum is the value of σ as predicted by Korst[40] for specified velocity ratio U_2/U_1.

In order to maintain σ maximum at the wall, the cosine function was written in the form

$$\cos \pi \left(\frac{\frac{R}{R_1} - \frac{r}{R_1}}{\frac{R}{R_1} - 1} \right) \quad \text{for} \quad \frac{r}{R_1} > 1 \tag{34}$$

This also yields minimum σ near the jet interface, as desired.

Thus, Equation (32), together with Equation (33) for σ, comprises the model proposed for the eddy viscosity ε_v. It still remains to formulate an expression for the eddy diffusivity ε_m in order to complete the set of equations presented in Chapter 2.

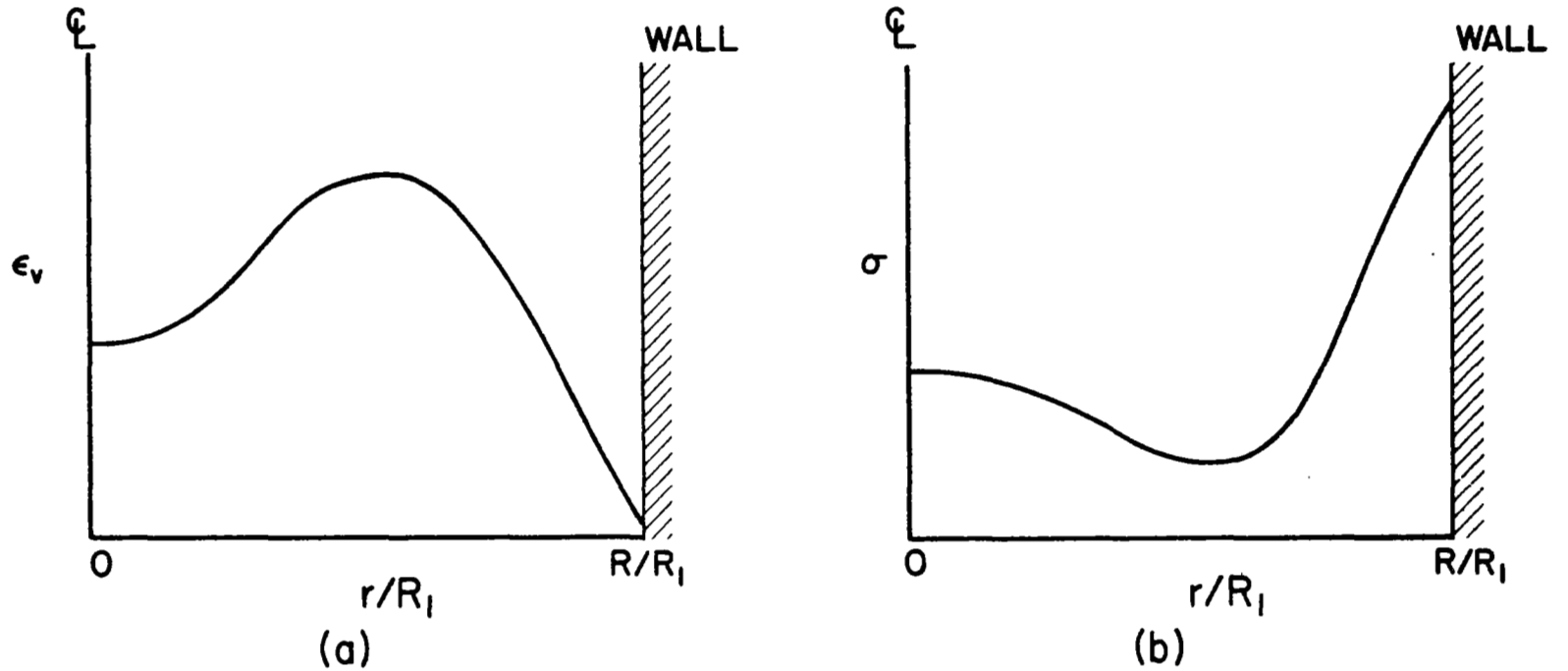

FIGURE 2. a) APPROXIMATE SHAPE OF EDDY VISCOSITY ϵ_v.
b) APPROXIMATE SHAPE OF NON DIMENSIONAL CORRELATING PARAMETER σ.

3.5 Some Remarks on the Turbulent Schmidt Number $N_{Sc,t}$ and the Eddy Diffusivity ε_m

In early analyses of mixing problems, it was often assumed that the turbulent Schmidt number $N_{Sc,t} = 1.0$, an assumption which simplifies the governing equations considerably. However, recent experiments indicate that $N_{Sc,t}$ may differ significantly from unity. Further, the experimental data of Forstall and Shapiro[32] show that $N_{Sc,t}$ remains constant at approximately 0.7 throughout the mixing region, so that the eddy diffusivity ε_m is merely a constant times the eddy viscosity ε_v. For gaseous components in binary mixing, the values of $N_{Sc,t}$ most frequently cited vary between 0.5 and 1.2. In the present work, $N_{Sc,t}$ is considered as a parameter and retained constant in the entire mixing region. Using suitable values for $N_{Sc,t}$ then yields the values for ε_m from calculated values of ε_v.

This completes the formulation of the boundary value problem. The solution is obtained by a finite difference method developed in Ref. 1. The results are presented and discussed in the next chapter.

CHAPTER 4

RESULTS AND DISCUSSION

4.1 Introduction

The analysis presented in Chapter 2, together with the eddy viscosity formulation proposed in Chapter 3, is used to obtain the flow field in a confined turbulent heterogeneous jet mixing system. The experimental data of Leithem, Kulik and Weinstein[2] were used to correlate the present analytical results and thereby arrive at appropriate values of the parameters in the expression for σ. Since the analysis uses the boundary layer equations, correlations were made only for the cases where U_2/U_1 and ρ_1/ρ_2 had values such that the flow may be adequately described by the turbulent boundary layer equations. Accordingly, four configurations of confined jet mixing were investigated. The values of the parameters for these four cases are summarized in Table I.

It may be appropriate at this stage to reflect briefly upon the validity of the boundary layer equations for confined mixing studies. Comparison of the laminar analysis with the concentration data of Wood[41] is shown in Fig. 3. The experimental measurements were made for an ethylene-nitrogen system ($\rho_1/\rho_2 \simeq 1.0$) with $U_2/U_1 = 1.18$ and $R_1/R = 0.563$.

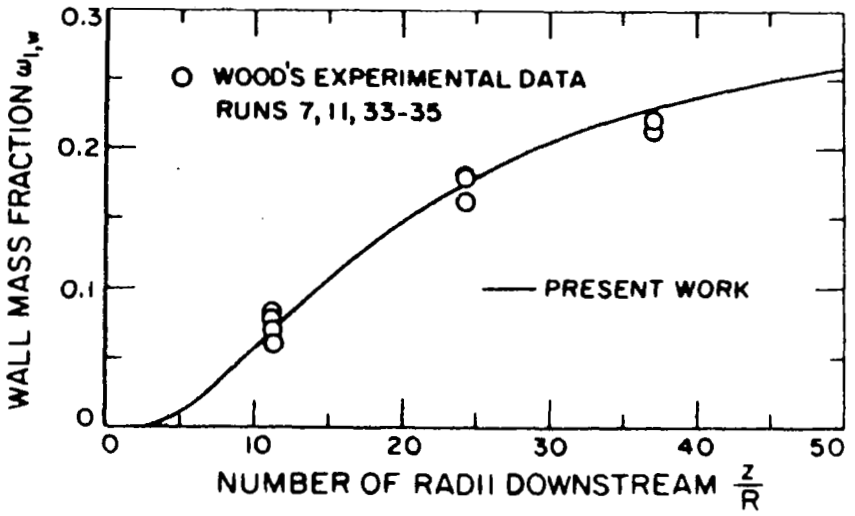

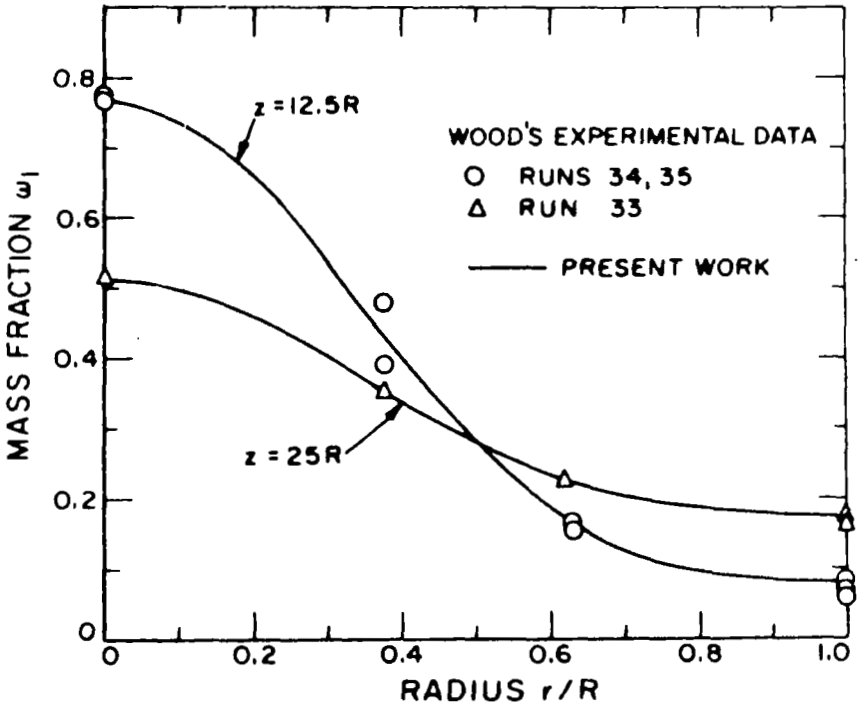

FIGURE 3. COMPARISON OF MASS FRACTION PROFILES WITH WOOD'S EXPERIMENTAL DATA.

Table I

Confined Jet Flow Systems*

Case	U_2/U_1	ρ_1/ρ_2	R_1/R	$U_2\rho_2/U_1\rho_1$	$N_{Re,2}/N_{Re,1}$	$N_{Sc,t}$
I	4.9	4.2	0.46	1.666	0.915	0.7
II	9.5	4.2	0.46	2.260	1.762	0.7
III	13.8	4.2	0.46	3.290	2.570	0.7
IV	5.8	1.0	0.46	5.800	6.700	1.0

Also, the non-dimensional centerline velocity is compared (Fig. 4) with the corresponding solution[42] of the Navier Stokes equations for the homogeneous cases with $R_1/R = 0.563$ and $U_2/U_1 = 4.0$, 3.0 and 2.0 As seen from Fig. 4, the deviation between the two solutions is limited to a small downstream distance; also, the agreement improves as the velocity ratio U_2/U_1 is decreased.

For the flow conditions in Table I, the consistency of the boundary layer equations was also checked by calculating the second order derivatives of the axial velocity v_z and the mass fraction ω_1. The axial derivatives were at least three

* $N_{Re,1}$ and $N_{Re,2}$ are based on the molecular viscosity for Freon and air respectively, since the experimental data were taken with a Freon-air system for the heterogeneous cases and with an air-air system for the homogeneous case.

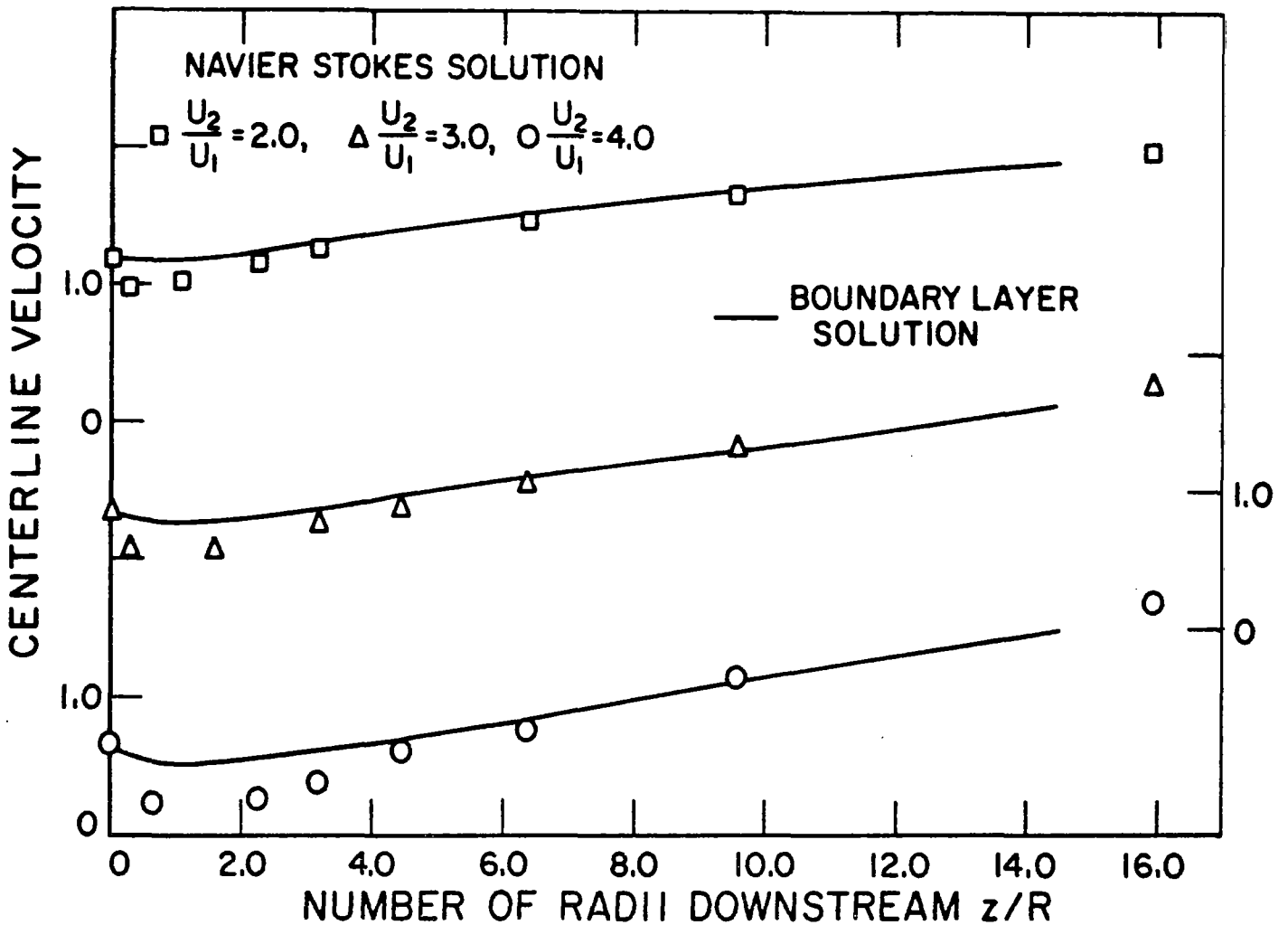

FIGURE 4. COMPARISON OF CENTERLINE VELOCITY WITH RESULTS OF REFERENCE 42.

orders of magnitude smaller than the corresponding transverse derivatives. Also, the radial velocity profiles showed only a low net radial flow. Similar checks were used by Weinstein and Todd[43] in order to show the consistency of the boundary layer equations for laminar unconfined mixing of streams with velocity ratio $U_2/U_1 = 100$ and density ratio $\rho_1/\rho_2 = 100$ which correspond to $U_2\rho_2/U_1\rho_1 = 1$. It must be mentioned here that, for a given radius ratio R_1/R, as the mass flux ratio $U_2\rho_2/U_1\rho_1$ increases, the radial velocities in the initial region increase. For Case IV with $U_2\rho_2/U_1\rho_1 = 5.8$, the radial velocities approach the same order of magnitude as the axial velocities, so that Case IV is approximately the limit of the range of validity of the present analysis.

Before discussing the results presented, it must be mentioned that attempts were also made to analyse the present problem using Ting and Libby's expression for eddy viscosity, Equation (31), as well as Alpinieri's formulation, Equation (30) for ϵ_v. It was found that the half radius $r_{1/2}$ appearing in these expressions for ϵ_v behaves quite differently for confined mixing under the present flow conditions ($U_2 > U_1$; $R_1 \approx 0.5R$) as compared to free jet mixing with $U_1 > U_2$. In fact, the conventional definition of the half-radius yields $r_{1/2} = 0$ beyond a certain axial distance z, so that Equations (30) and (31) predict $\epsilon_v = 0$ for the region downstream of this value of z. This behavior of $r_{1/2}$, which may be due to the global continuity of the flow and the effect of the boundary layer developing at the confining walls, raises the question of the validity of using $r_{1/2}$ in the eddy viscosity

models for confined jet mixing. An alternate measure of the jet width, as for example one based on the mass fraction rather than velocities, may perhaps be used more adequately in place of the half radius $r_{1/2}$ in Equations (30) and (31).

Further efforts were directed to analyse the present problem using only the proposed model for the eddy viscosity, Equation (32). This model, with constant σ was used successfully by Emmons[20] to correlate his analysis with the experimental data of Shapiro and Forstall[32] in the similarity region of a homogeneous mixing system with $R_1/R = 1/16$ and U_2/U_1 between 0.2 and 0.75. In the present analysis of heterogeneous mixing configurations, with $R_1/R = 0.46$ and $U_2 > U_1$, σ is a radially varying non-dimensional parameter. The idea of varying the empirical constant in an eddy viscosity model was also used by Donaldson and Gray[44] in their investigation of unconfined heterogeneous mixing of compressible streams. Starting with Prandtl's classical model, Equation (26), for constant density mixing, Donaldson and Gray used a continuously varying k in order to correlate their analysis with experimental data.

4.2 Discussion of Present Results

Figures 5 through 8 show the comparison of the velocity and the density profiles of the present results with experimental data for the four cases listed in Table I. For the homogeneous Case IV with $\rho_1/\rho_2 = 1.0$, the density profiles are not presented because

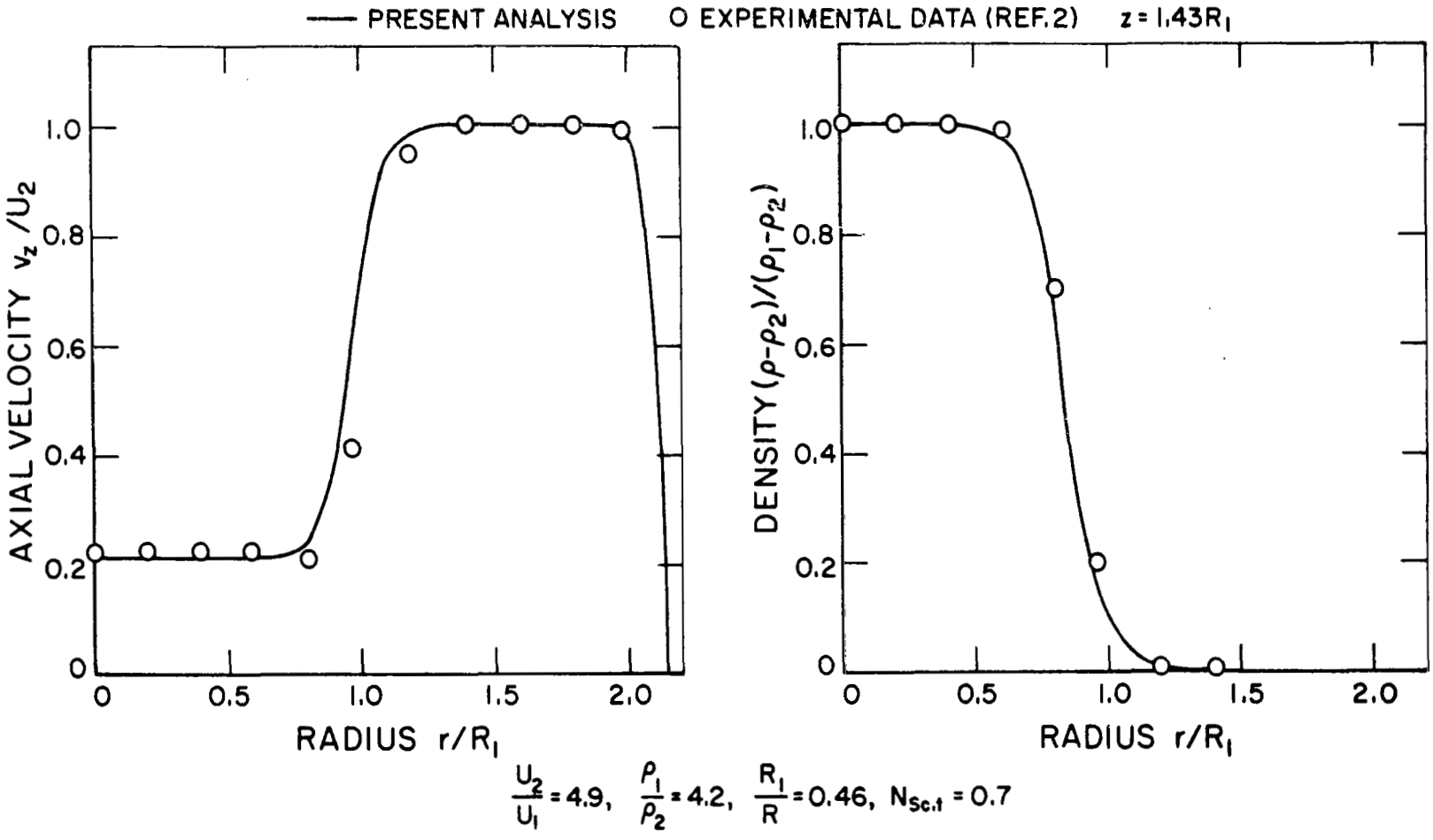

FIGURE 5. COMPARISON OF VELOCITY AND DENSITY PROFILES WITH EXPERIMENTAL DATA OF REFERENCE 2, CASE 1.

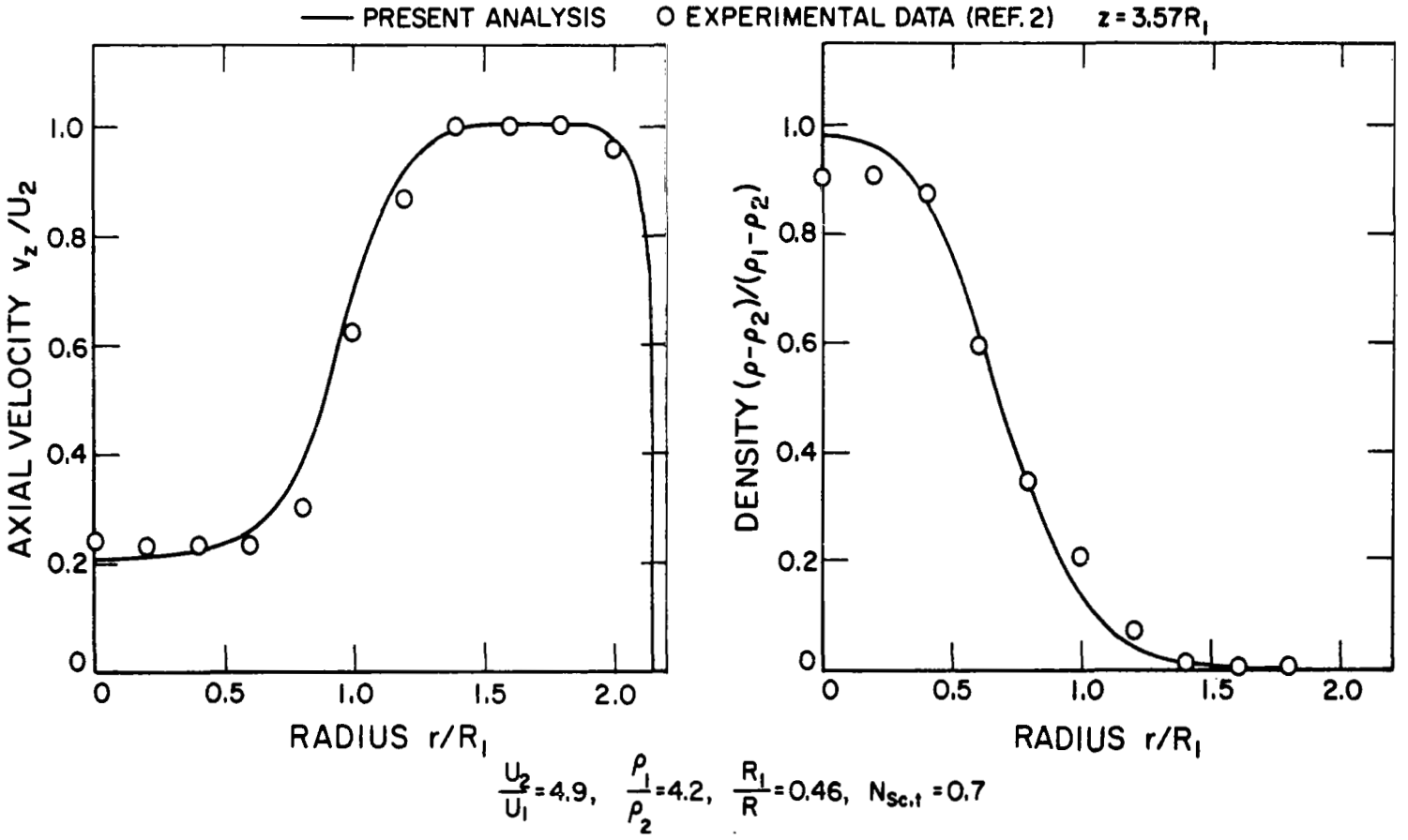

FIGURE 5 continued. COMPARISON OF VELOCITY AND DENSITY PROFILES WITH EXPERIMENTAL DATA OF REFERENCE 2, CASE 1.

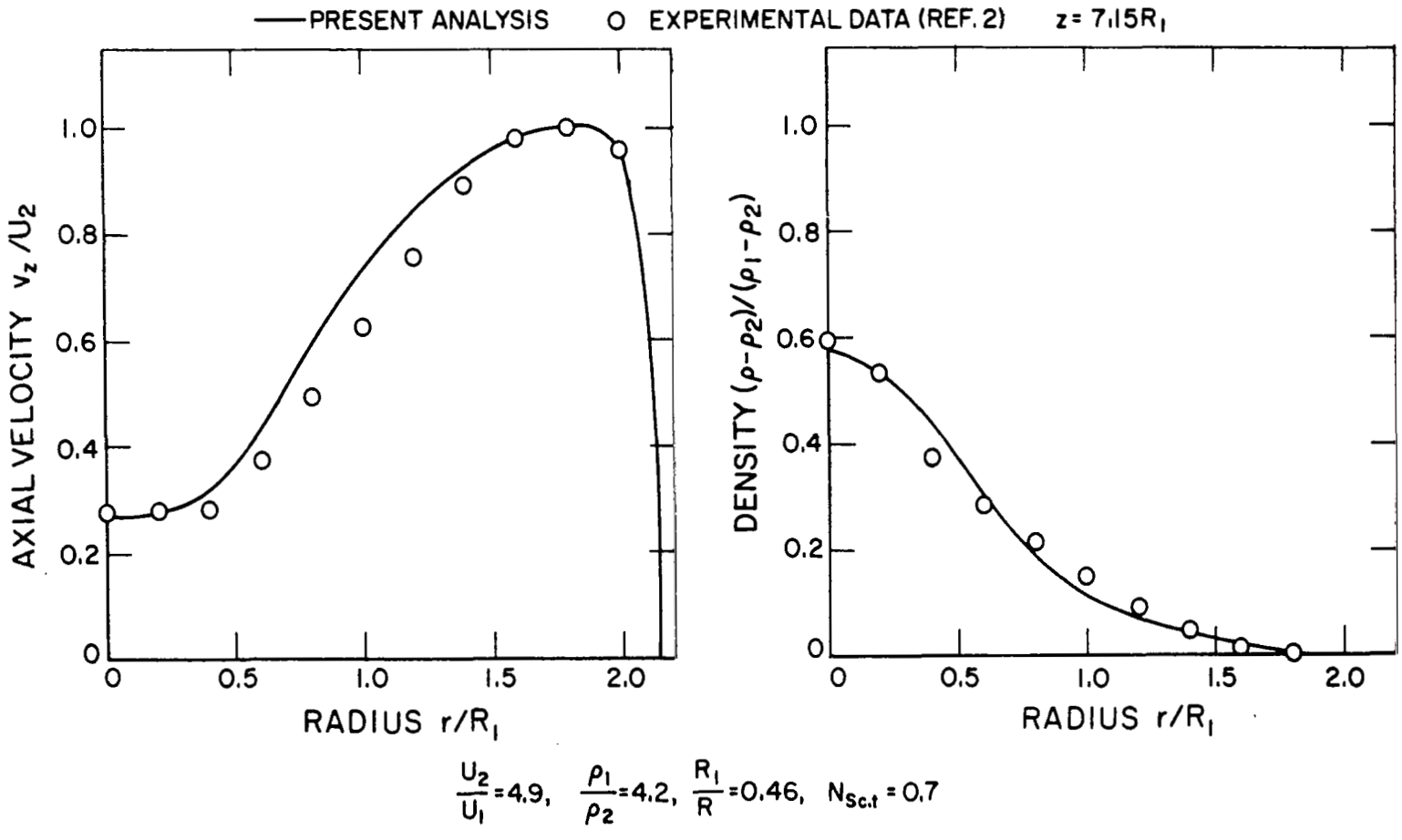

FIGURE 5 continued. COMPARISON OF VELOCITY AND DENSITY PROFILES WITH EXPERIMENTAL DATA OF REFERENCE 2, CASE 1.

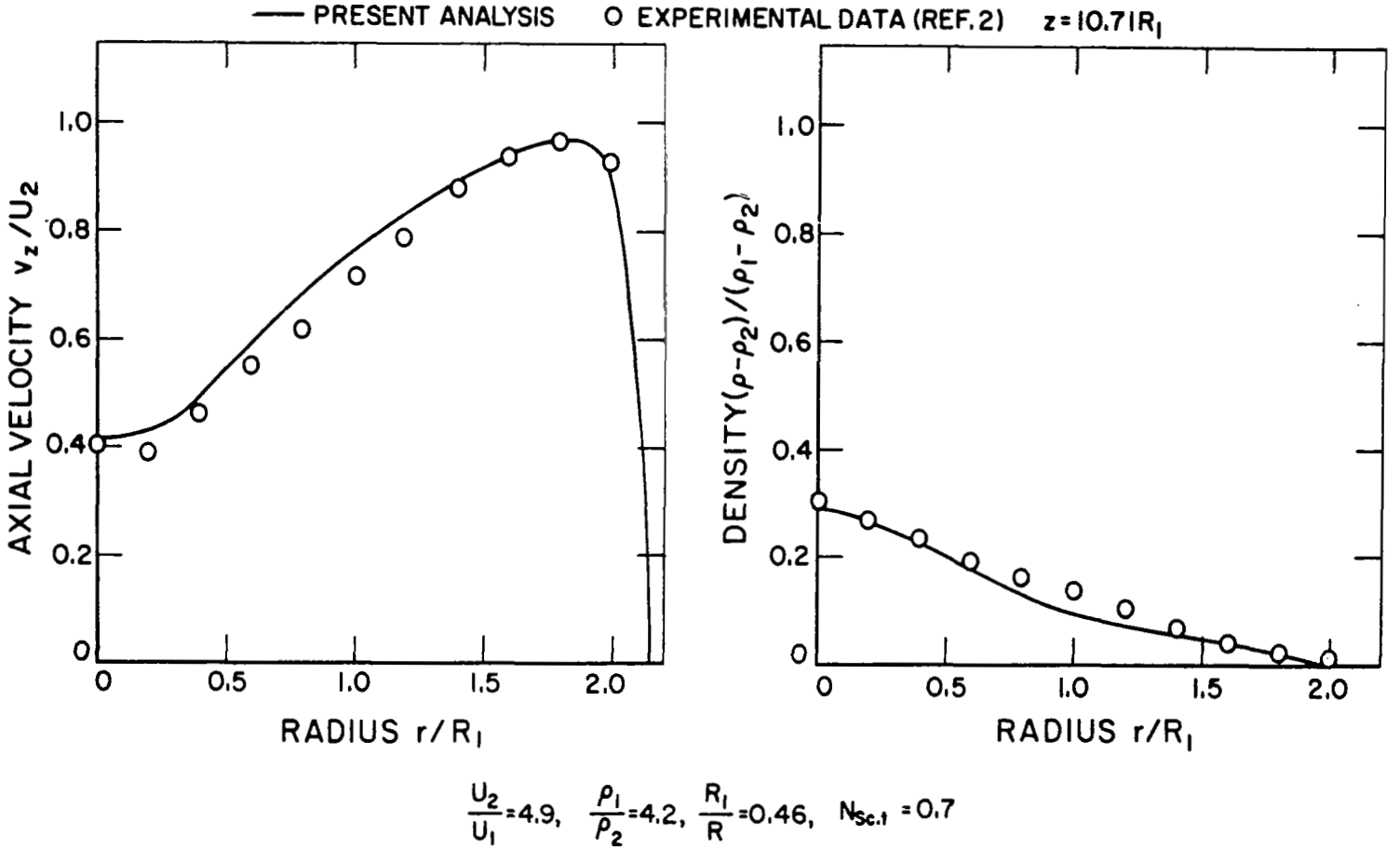

FIGURE 5 concluded. COMPARISON OF VELOCITY AND DENSITY PROFILES WITH EXPERIMENTAL DATA OF REFERENCE 2, CASE 1.

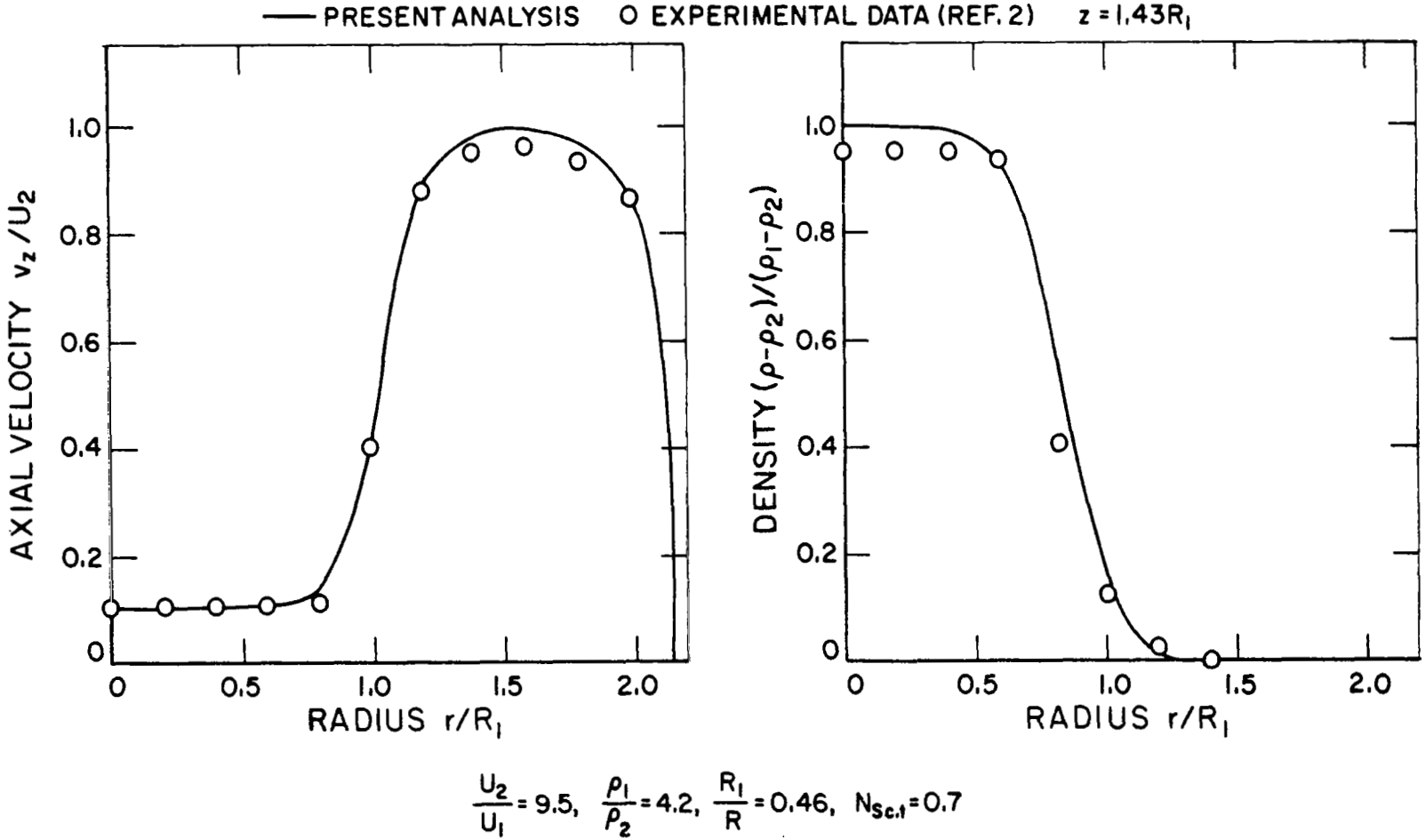

FIGURE 6. COMPARISON OF VELOCITY AND DENSITY PROFILES WITH EXPERIMENTAL DATA OF REFERENCE 2, CASE II.

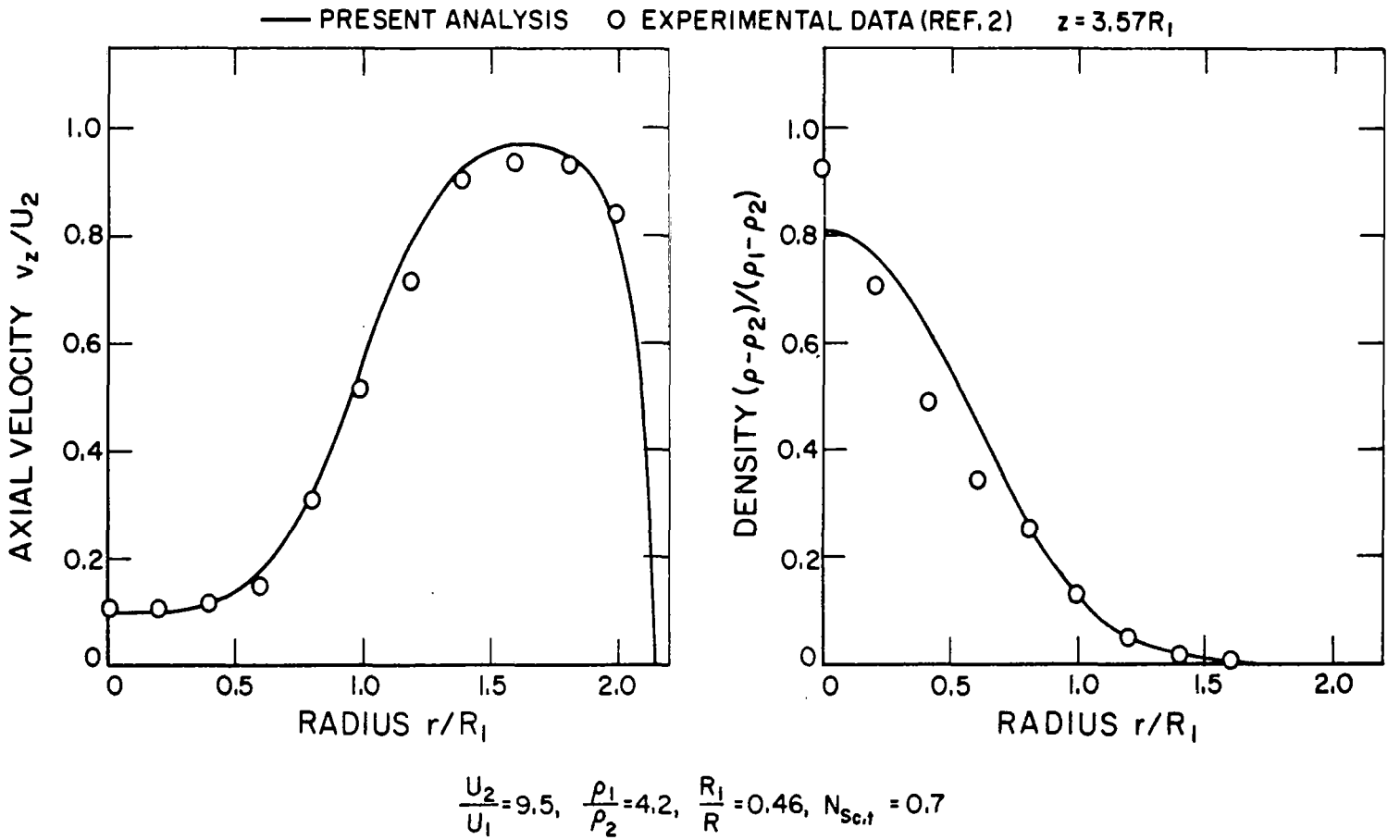

FIGURE 6 continued. COMPARISON OF VELOCITY AND DENSITY PROFILES WITH EXPERIMENTAL DATA OF REFERENCE 2, CASE II.

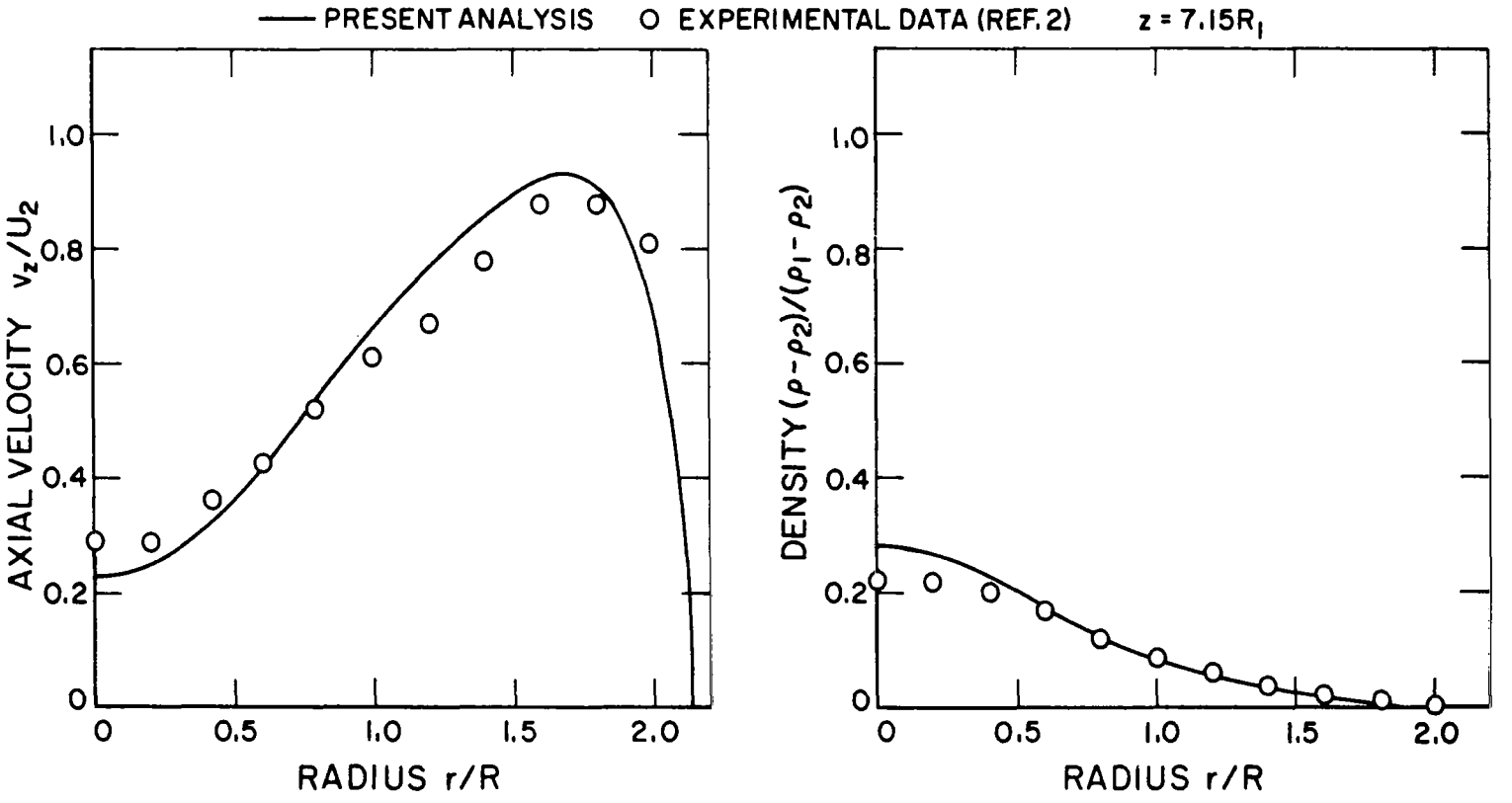

FIGURE 6 continued. COMPARISON OF VELOCITY AND DENSITY PROFILES WITH EXPERIMENTAL DATA OF REFERENCE 2, CASE II.

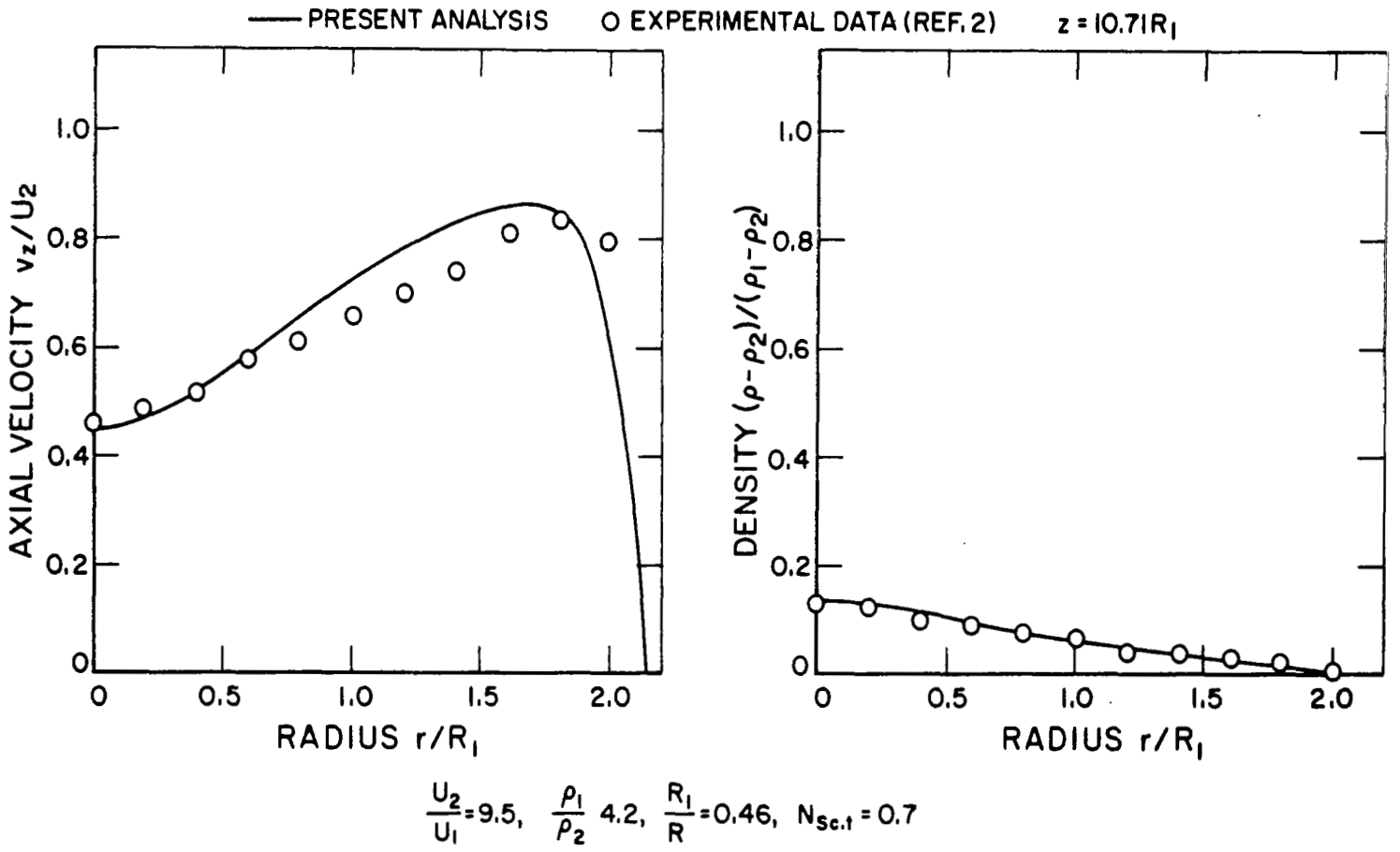

FIGURE 6 concluded. COMPARISON OF VELOCITY AND DENSITY PROFILES WITH EXPERIMENTAL DATA OF REFERENCE 2, CASE II.

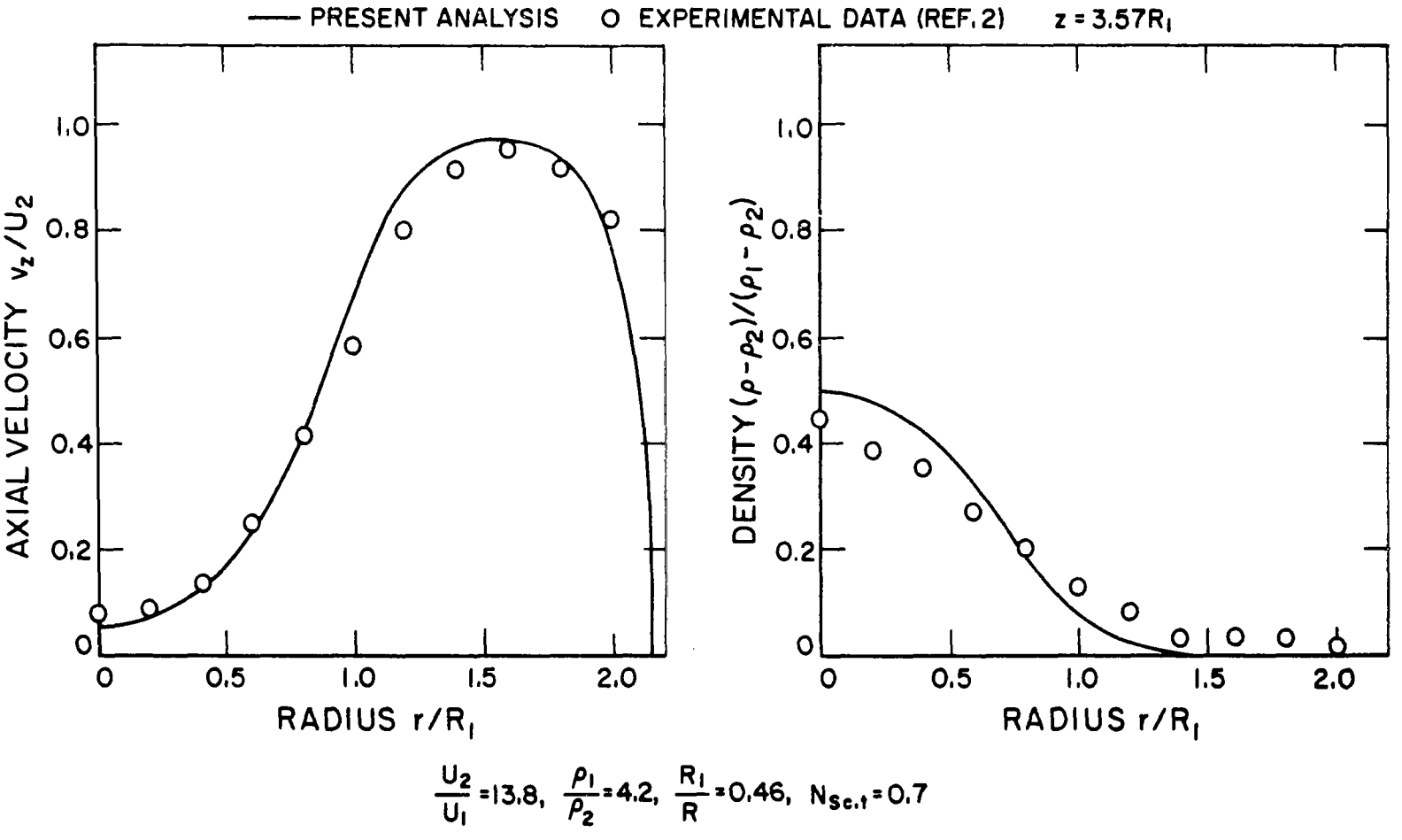

FIGURE 7. COMPARISON OF VELOCITY AND DENSITY PROFILES WITH EXPERIMENTAL DATA OF REFERENCE 2, CASE III.

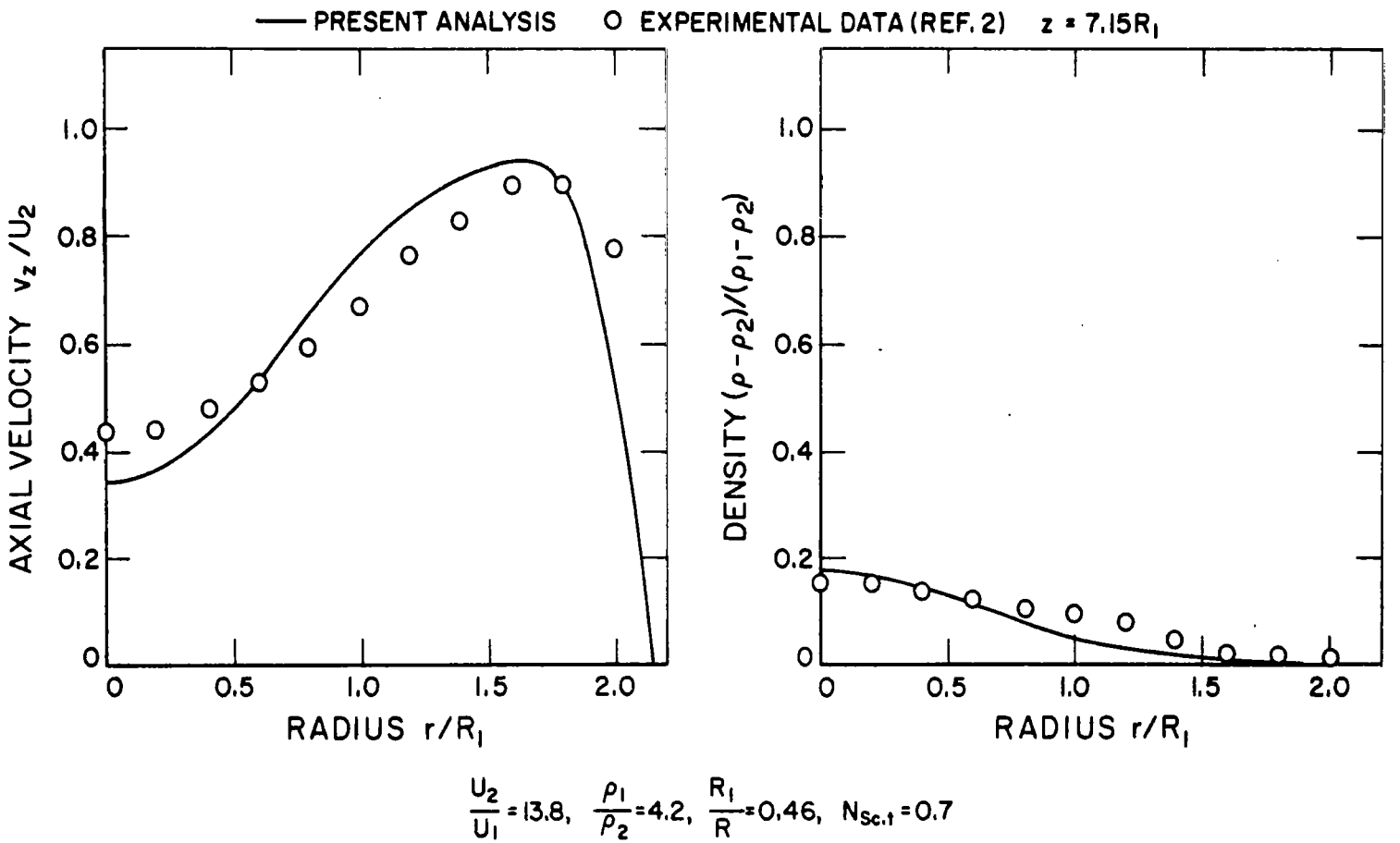

FIGURE 7 continued. COMPARISON OF VELOCITY AND DENSITY PROFILES WITH EXPERIMENTAL DATA OF REFERENCE 2, CASE III.

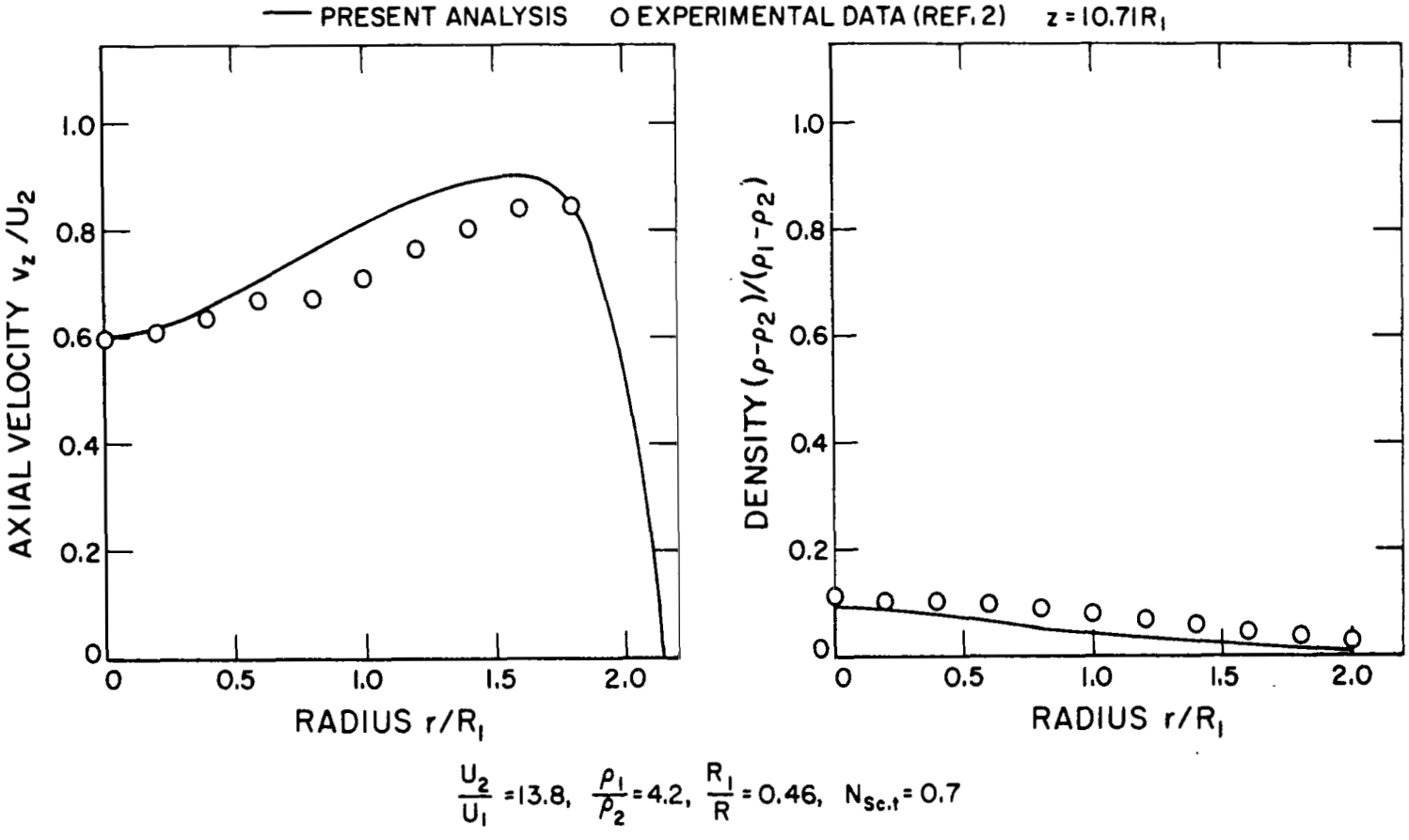

FIGURE 7 concluded. COMPARISON OF VELOCITY AND DENSITY PROFILES WITH EXPERIMENTAL DATA OF REFERENCE 2, CASE III.

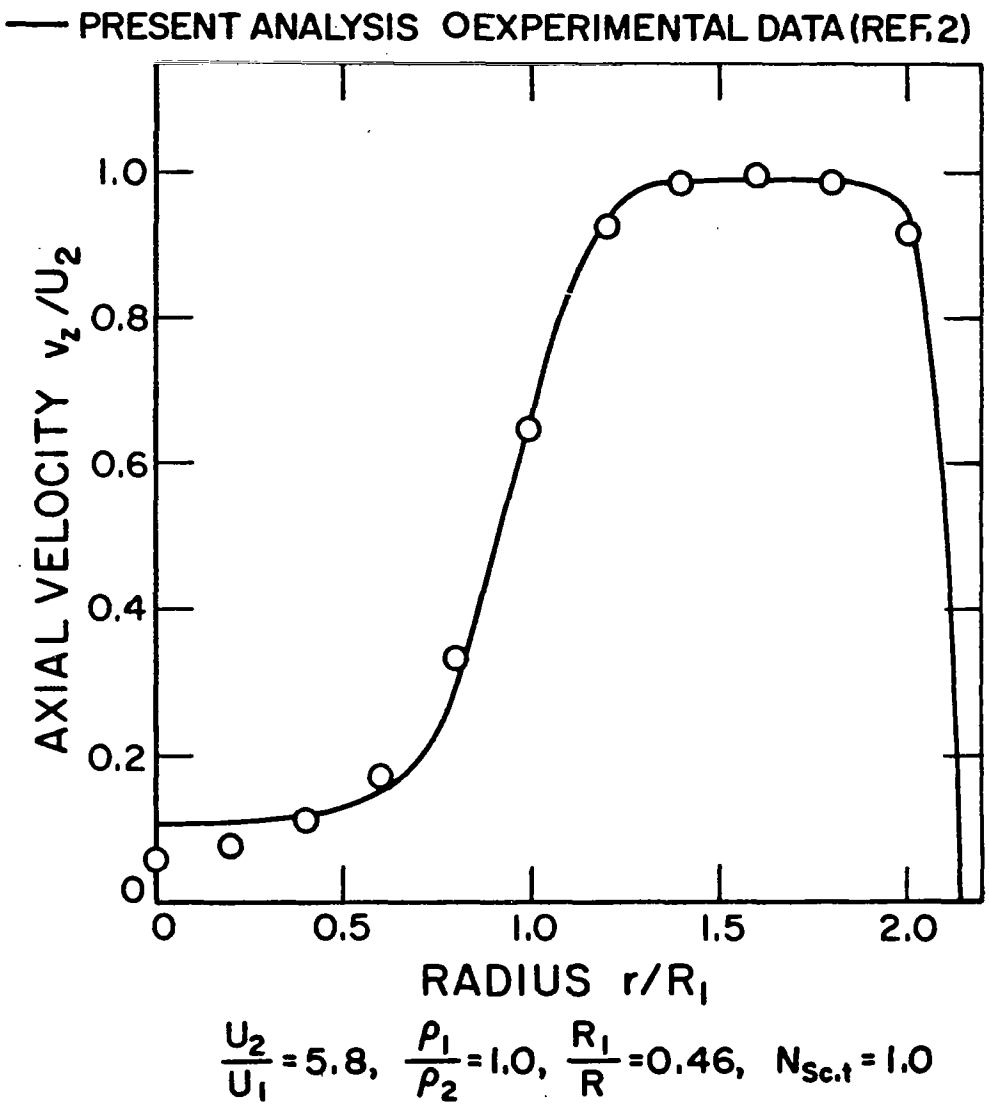

FIGURE 8. COMPARISON OF VELOCITY PROFILES WITH EXPERIMENTAL DATA OF REFERENCE 2, CASE IV.

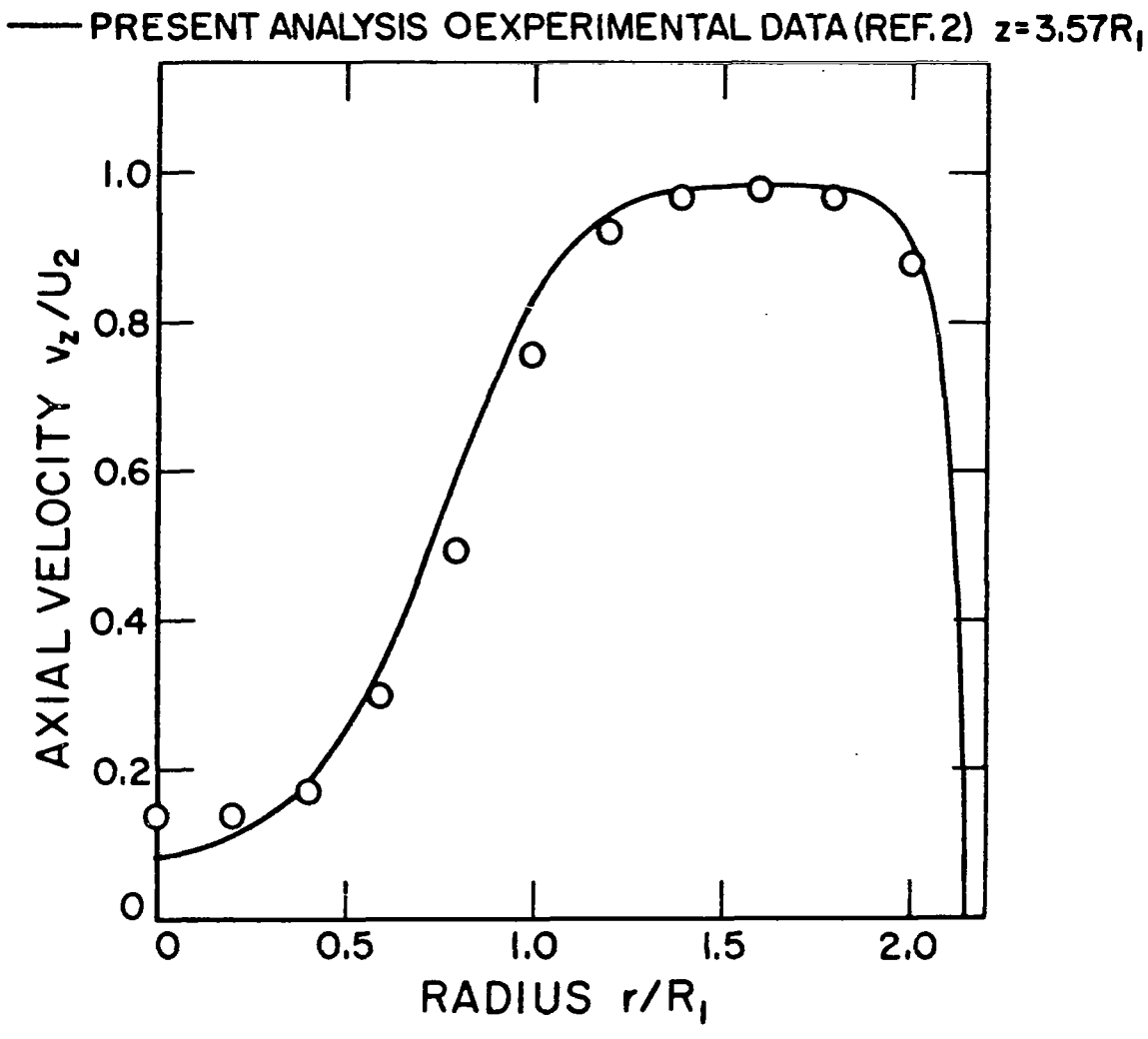

$$\frac{U_2}{U_1} = 5.8, \quad \frac{\rho_1}{\rho_2} = 1.0, \quad \frac{R_1}{R} = 0.46, \quad N_{Sc,t} = 1.0$$

FIGURE 8 continued. COMPARISON OF VELOCITY PROFILES WITH EXPERIMENTAL DATA OF REFERENCE 2, CASE IV.

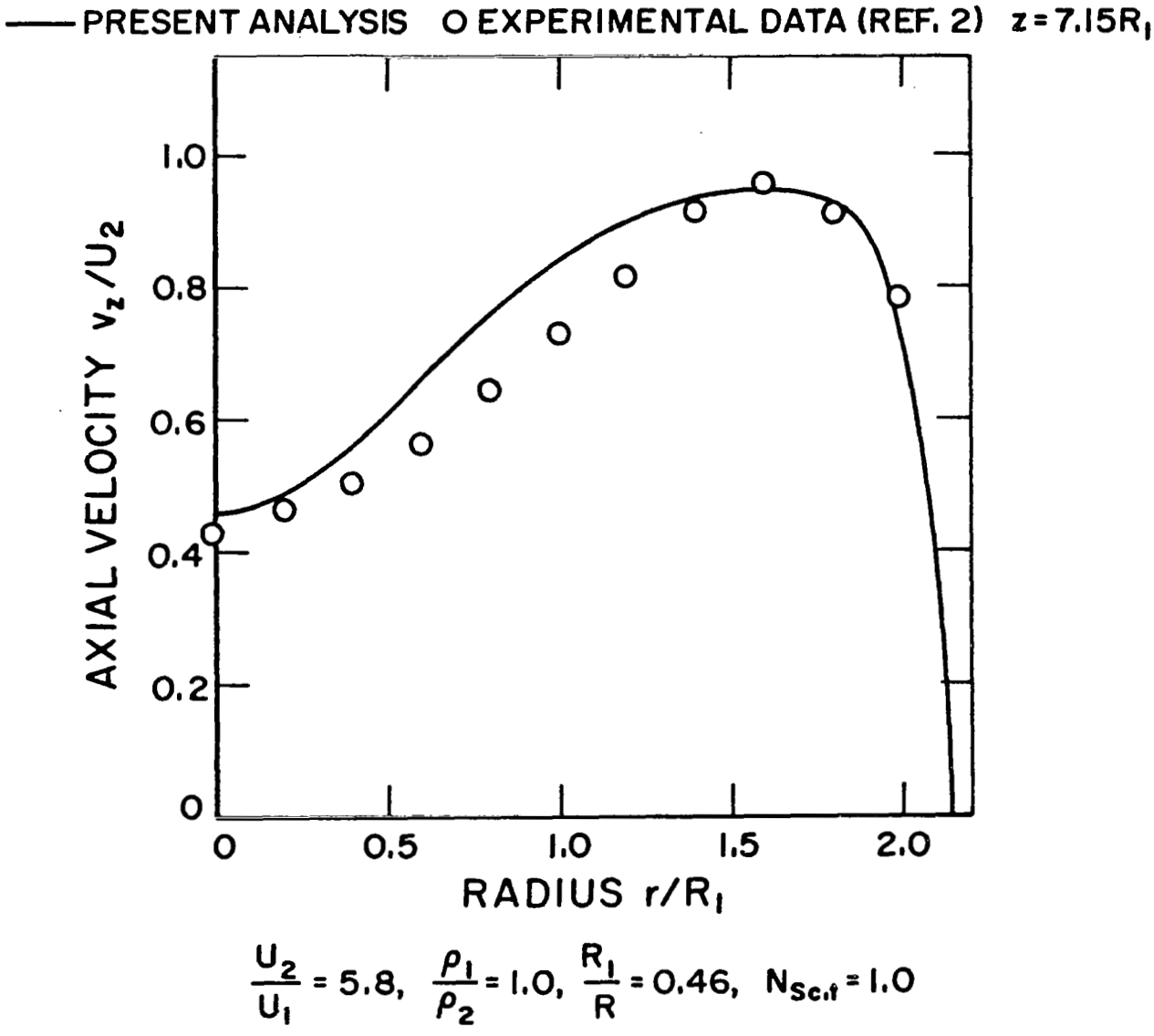

$$\frac{U_2}{U_1} = 5.8, \quad \frac{\rho_1}{\rho_2} = 1.0, \quad \frac{R_1}{R} = 0.46, \quad N_{Sc,f} = 1.0$$

FIGURE 8 continued. COMPARISON OF VELOCITY PROFILES WITH EXPERIMENTAL DATA OF REFERENCE 2, CASE IV.

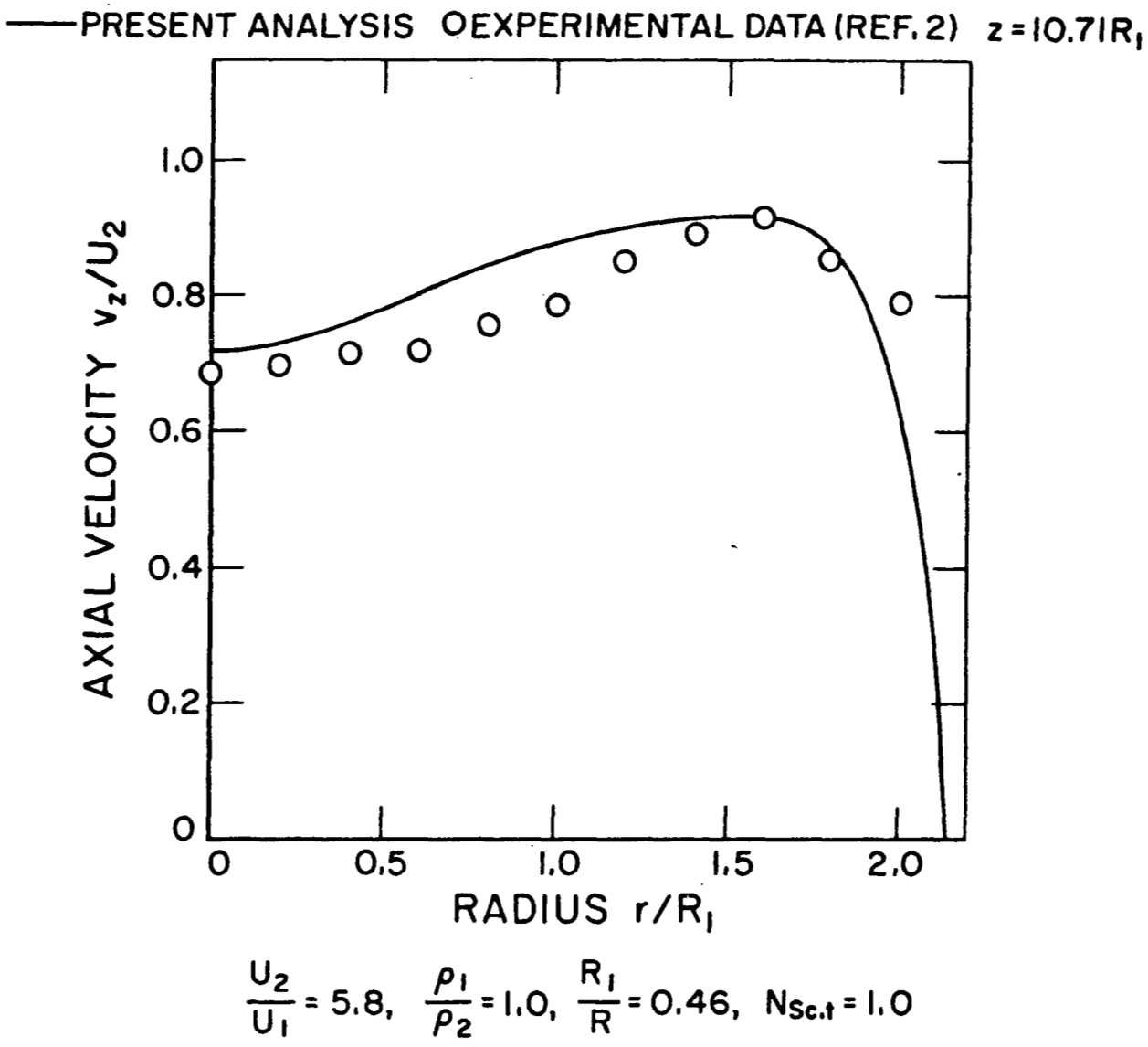

FIGURE 8 concluded. COMPARISON OF VELOCITY PROFILES WITH EXPERIMENTAL DATA OF REFERENCE 2, CASE IV.

the density in this case is everywhere uniform. The velocity profiles used at the inlet section $z = 0$ were those obtained in the experiments. It must be noted here that calculation of mass flow rate using the experimental velocity and density profiles showed that the total mass flow rate in each case varied by about 10 to 15 percent in the initial region.

The results are presented for several downstream distances, and with references to Fig. 1, they are for the initial region. It can be seen from these results that an increase in the velocity ratio U_2/U_1 leads to faster mixing and development of the flow. Similar effect is also observed as ρ_1/ρ_2 is reduced from 4.2 in Case I to $\rho_1/\rho_2 = 1.0$ in Case IV. The ratios U_2/U_1 and ρ_1/ρ_2 were varied by essentially varying U_1 and ρ_1 respectively.

In the confined turbulent mixing process, the static pressure is expected to increase with downstream distance z. Also, the viscous effects at the confining wall cause a decrease in the pressure with increasing axial distance z. The result is a negative or a positive axial pressure gradient dp/dz depending on whether the viscous effects at the wall dominate or the effects of the mixing process are more predominant. The variation of the normalized axial pressure gradient is presented in Fig. 9 for the four cases investigated. The axial pressure gradient dp/dz in each case has been normalized with respect to its corresponding value for fully developed turbulent pipe flow. Negative values of normalized pressure gradient indicate positive values of the actual pressure gradient dp/dz since the normalizing value of the

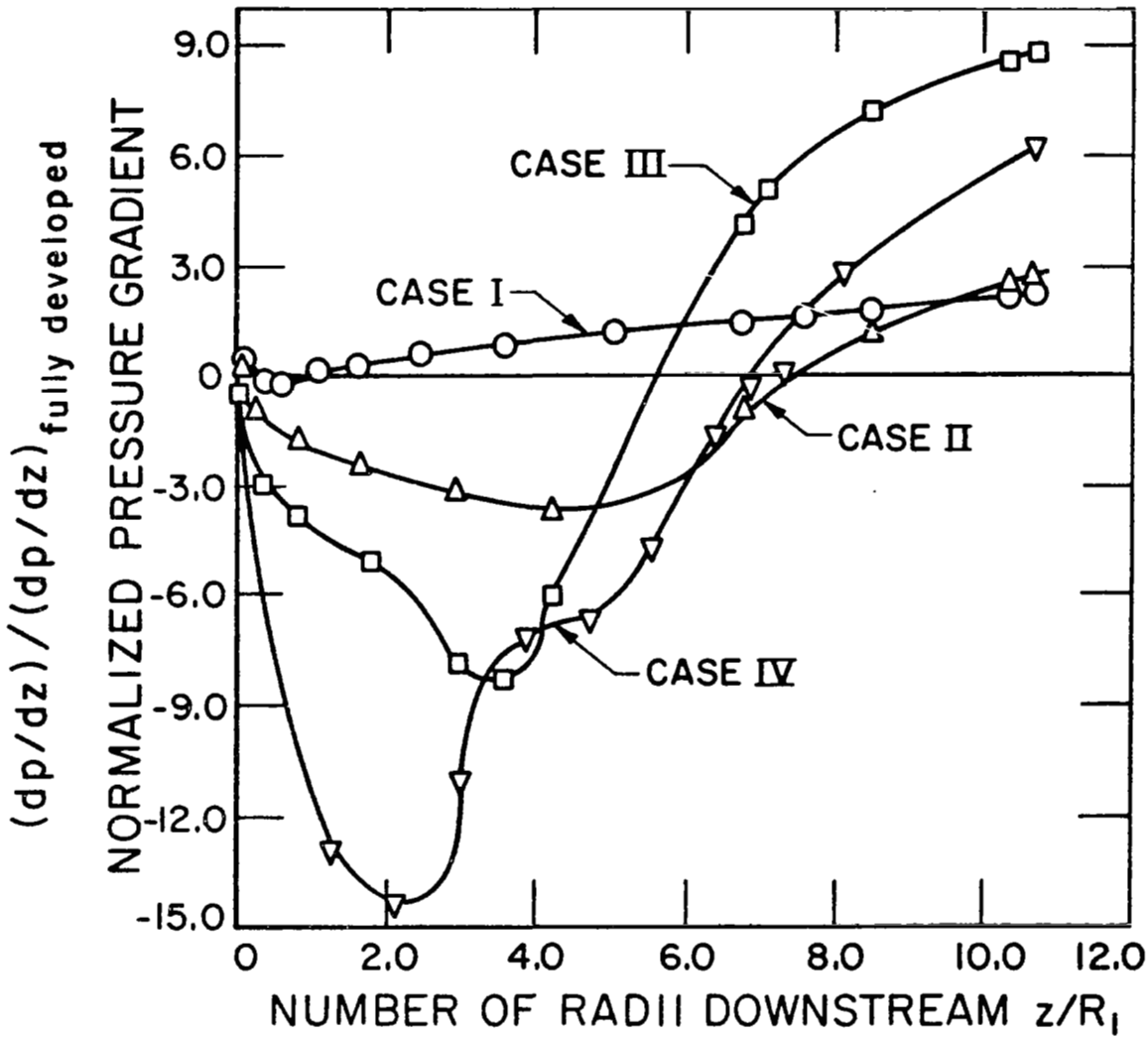

FIGURE 9. NORMALIZED AXIAL PRESSURE GRADIENT VS. DOWNSTREAM DISTANCE, FOR CASES I, II, III, IV.

pressure gradient is negative. Thus, it is seen from Fig. 9 that positive pressure gradient prevails in all the four cases studied. The magnitude of this adverse dp/dz decreases with decrease in the ratio $U_2\rho_2/U_1\rho_1$. The presence of a positive pressure gradient leads to a reduction of the axial velocity v_z particularly near the centerline. The value of the minimum centerline axial velocity $v_{z,c}$ decreases with increase in the velocity ratio U_2/U_1. For some value of U_2/U_1, the axial velocity will approach zero and further increase in U_2/U_1 will yield negative axial velocities. This is the onset of recirculation phenomenon wherein the entrainment capacity of the faster moving outer stream exceeds the amount of fluid supplied by the low velocity inner stream. The outer stream then recirculates some of its own fluid to meet its entrainment requirements. The present analysis is no longer be valid as the parameters of the problem approach the values for which recirculation occurs. It must be mentioned here that for Case III which has the maximum velocity ratio investigated, $U_2/U_1 = 13.8$, the minimum non-dimensional centerline axial velocity $v_{z,1}$ is approximately 0.04. Therefore, the largest value of $U_2/U_1 = 13.8$ presented in Table I, where $\rho_1/\rho_2 = 4.2$, is approximately the maximum velocity ratio U_2/U_1 for which the present analysis is valid.

Figure 10 presents the typical radial variations of ε_v and $\rho\varepsilon_v$ for the cases studied. The increase of eddy viscosity ε_v with axial distance z is in conformity with the experimental

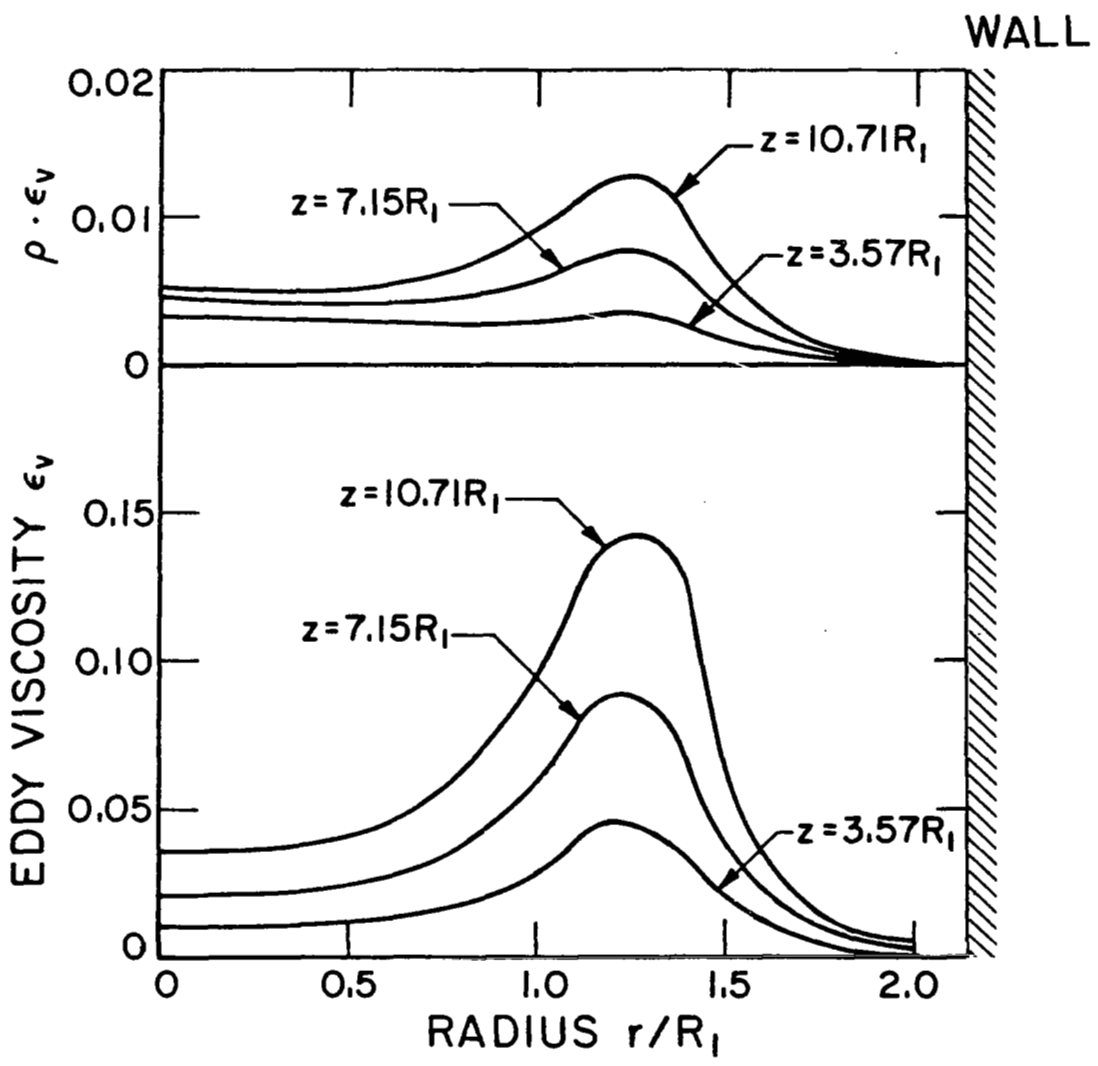

FIGURE 10. TYPICAL RADIAL PROFILES OF ϵ_v AND $\rho\epsilon_v$.

results of Boehman.[45] It must be reported here that, for the present analysis, attempts were also made to replace the variation of ε_v with z by an axial variation of the form z^n where $n < 1$. This would increase the value of the eddy viscosity ε_v for $z < 1$ and decrease it for $z > 1$. The corresponding results obtained showed no improvement, so that the variation of ε_v with z was retained as in Equation (32). However, the attempts to use z^n, $n < 1$, lead the author to believe that better correlation may be obtained by shifting the crossing point of the z^n, $n < 1$, curve with the z^1 line from the value $z = 1$ to some value $z < 1$. (See sketch shown below.) It may be worth investigating the axial variation of ε_v in the form $(z/L)^n$ where $n < 1$ and the constant L depends on the exponent n and on the value of z where the crossing point of the $(z/L)^n$ curve with the z^1 line is desired to be located.

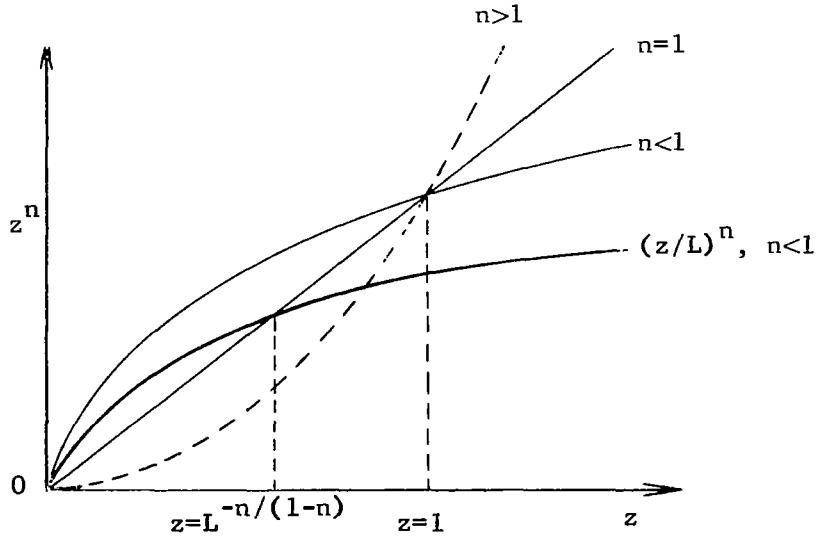

The sharp decrease in the eddy viscosity values on the right of the peak of the ϵ_v curves in Fig. 10 corresponds to the region where the velocity profiles show a plateau and where the Reynolds stress tends towards zero. This sharp decrease manifests itself through the positive curvature of the ϵ_v curves in this region. On the other hand, in the same region, the ϵ_v curve for fully developed turbulent pipe flow is of negative curvature. This disagreement should not be surprising since the eddy viscosity formulation used in the present analysis was intended for the initial mixing region only. It is also interesting to note that the values of ϵ_v in the mixing region are very much larger than those for single pipe flow. In Fig. 10, the ϵ_v curves for the region between $r/R_1 = 2.00$ and the wall are not shown, since the values there are very small compared to the peak values.

The dynamic eddy viscosity $\rho\epsilon_v$ is found to be a relatively weak function of the transverse coordinate r, so that $\rho\epsilon_v$ may be considered to depend only on the axial distance z. This was also observed by Alpinieri[33] to be true for the correlation of his analysis with his experimental data for a carbon dioxide-air system and a hydrogen-air system with $R_1/R = 0.25$ and U_1/U_2 between 0.47 and 1.25. It must be noted here that, in the governing differential equations presented in Chapter 2, the coefficients of the molecular viscosity μ and the molecular diffusivity D_{12} were written separately from the eddy viscosity $\rho\epsilon_v$ and the eddy diffusivity $\rho\epsilon_m$, respectively. Therefore, the eddy viscosity ϵ_v and the eddy diffusivity ϵ_m must approach zero at the wall. To circumvent this situation the sum of $(\mu + \rho\epsilon_v)$ was replaced by an equivalent total of $\rho\epsilon_v$ and $(D_{12} + \epsilon_m)$ was replaced by $\rho\epsilon_v/N_{Sc,t}$. Consequently, the eddy viscosity ϵ_v was required to decrease to the molecular viscosity value near the wall. The corresponding value required for σ was

obtained by using a different value A_1' in the region near the wall for the coefficient A_1 of the exponential cosine function. Matching the values of σ near the jet interface $r/R_1 = 1.0$ yields the following expression for σ for $r/R_1 > 1.0$.

$$\sigma = e^{r/R_1}\left[A_1' + A_1' \cos \pi\left(\frac{\frac{R}{R_1} - \frac{r}{R_1}}{\frac{R}{R_1} - 1}\right) - A_1\right] + A_2$$

$$\text{for } 1 < \frac{r}{R_1} \leq \frac{R}{R_1} \qquad (35)$$

Thus, the non-dimensional parameter σ appearing in Equation (32) for the eddy viscosity ε_v, is given by Equation (33) for $0 \leq \frac{r}{R_1} \leq 1$ and by Equation (35) for $1 < \frac{r}{R_1} \leq \frac{R}{R_1}$. The values of the parameters in these expressions for σ are obtained from the correlations for the four cases of Table 1 and are shown in Fig. 11. The variation of these parameters with mass flux ratio $U_2\rho_2/U_1\rho_1$ leads to the following interesting interpretation for the expression used for σ. The constant part A_2 of σ, may be considered to correspond to unconfined mixing, whereas the variable part of σ accounts for the confined mixing. As the velocity ratio U_2/U_1 increases, but remains below the value for which recirculation occurs, the effect of the variable part in σ diminishes and the constant part A_2 dominates and approaches the value of 12 established for free jet mixing with a quiescent atmosphere.

From Equation (33) and the results presented in Fig. 11, it is also seen that the presence of a moving secondary stream requires a larger mean value of σ. This result for confined mixing is in accordance with Korst's[40] experimental results for two-dimensional free mixing. Further, as the velocity ratio U_2/U_1 increases or the density ratio ρ_1/ρ_2 decreases, the mean value of σ decreases. Similar conclusions have been also obtained from the experiments of Baker and Weinstein[46] and Korst.[40]

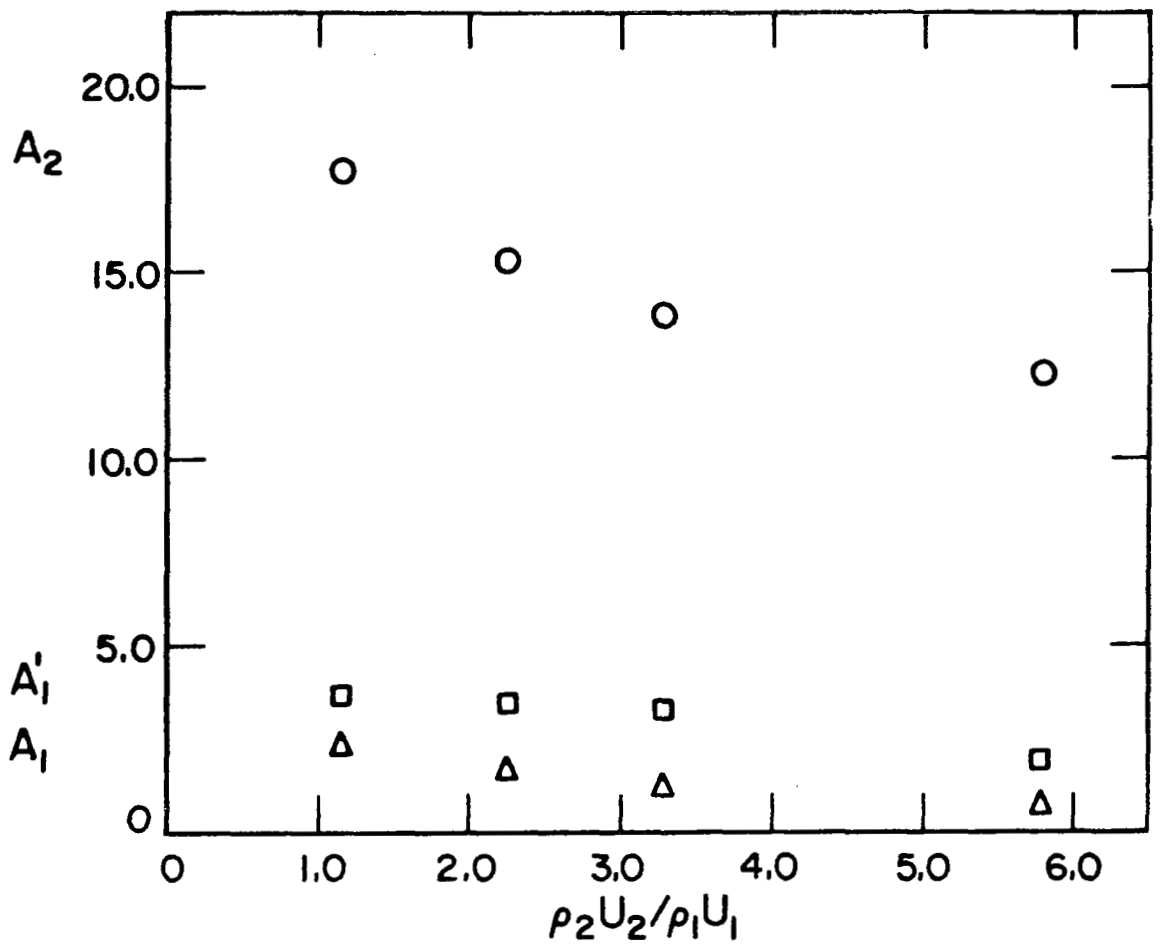

FIGURE 11. PARAMETERS APPEARING IN EQUATIONS (33) AND (35) VS. $\rho_2 U_2/\rho_1 U_1$.

As seen from Table I, the radius ratio R_1/R is equal to 0.46 for the four cases studied. Therefore, it must be noted that the present formulation for σ has been checked to be appropriate for confined jet mixing with this radius ratio only.

As mentioned in Section 3.4, a constant value of 0.7 was used for the turbulent Schmidt number $N_{Sc,t}$ in the present analysis. Results were also obtained with $N_{Sc,t} = 0.6$ and $N_{Sc,t} = 0.8$. It was found that the radial profiles of the axial velocities were insensitive to these small changes in the value of the turbulent Schmidt number. Similar observations have also been reported by Alpinieri.[33] In the present investigation, however, the variations in the density profiles due to changes in $N_{Sc,t}$ were not negligible. The results for $N_{Sc,t}$ other than 0.7 have not been presented.

It must be recalled that, for the present study, experimental data were available in the initial region only; hence, the analysis was correlated with experiment in this region only. However, it may be interesting to see the results of the analysis in the main region far downstream. These are presented in Fig. 12 for the four cases investigated. The corresponding fully developed theoretical velocity profile for each case is also shown in the same figure. Of course, no deductions may be made on the basis of these results. Experimental data in the main region of confined mixing are needed in order to make any conclusive statements regarding the use of the present eddy viscosity formulation in this region.

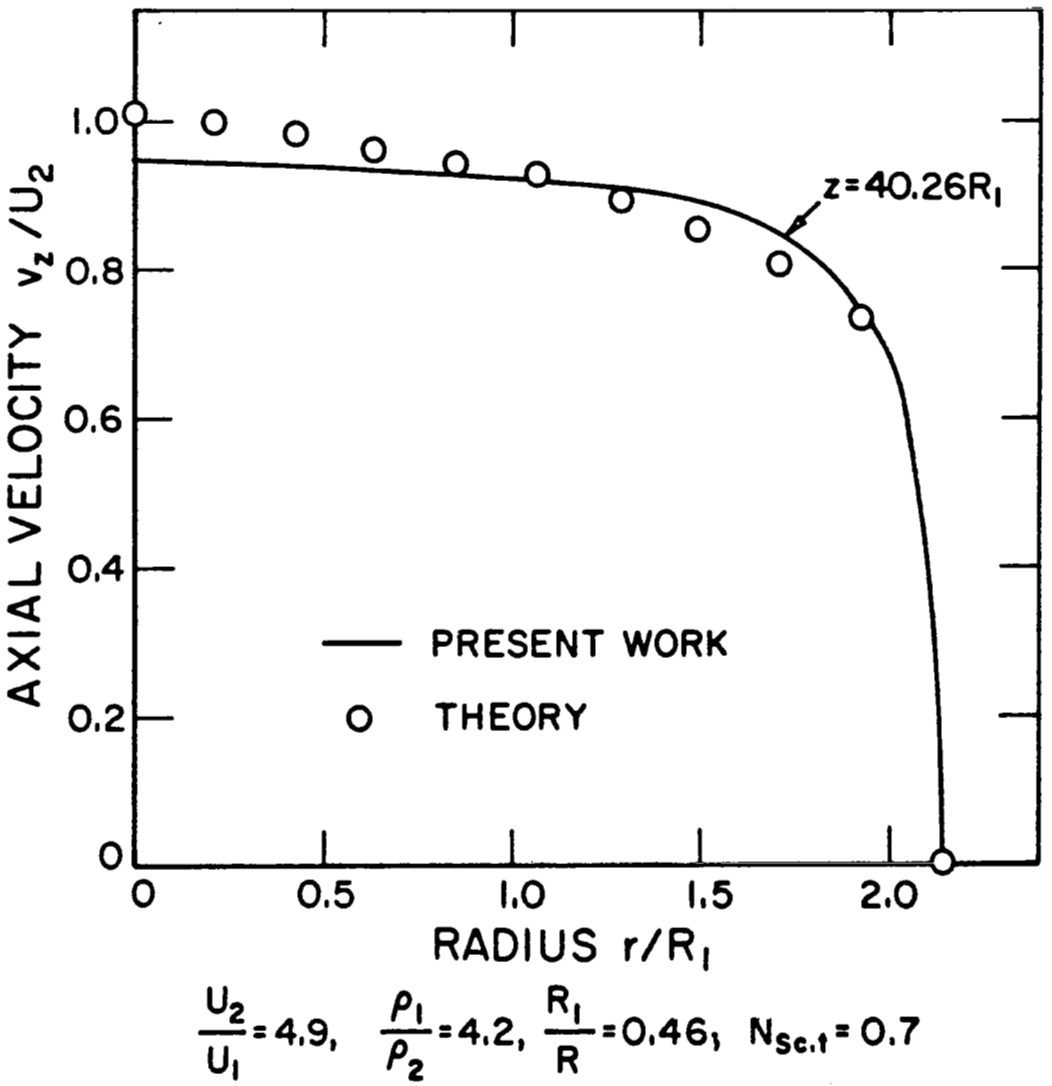

FIGURE 12. FULLY DEVELOPED AXIAL VELOCITY PROFILES.

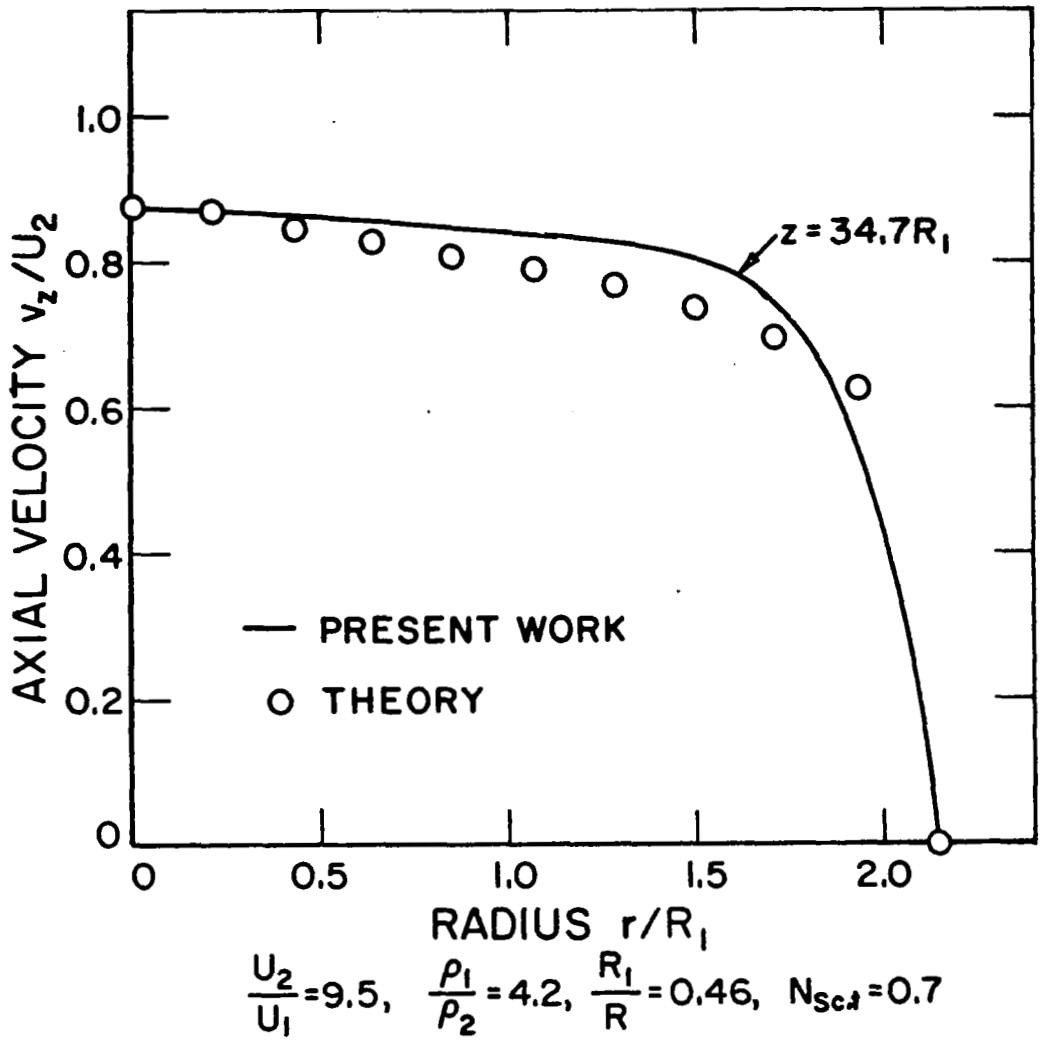

FIGURE 12 continued. FULLY DEVELOPED AXIAL VELOCITY PROFILES.

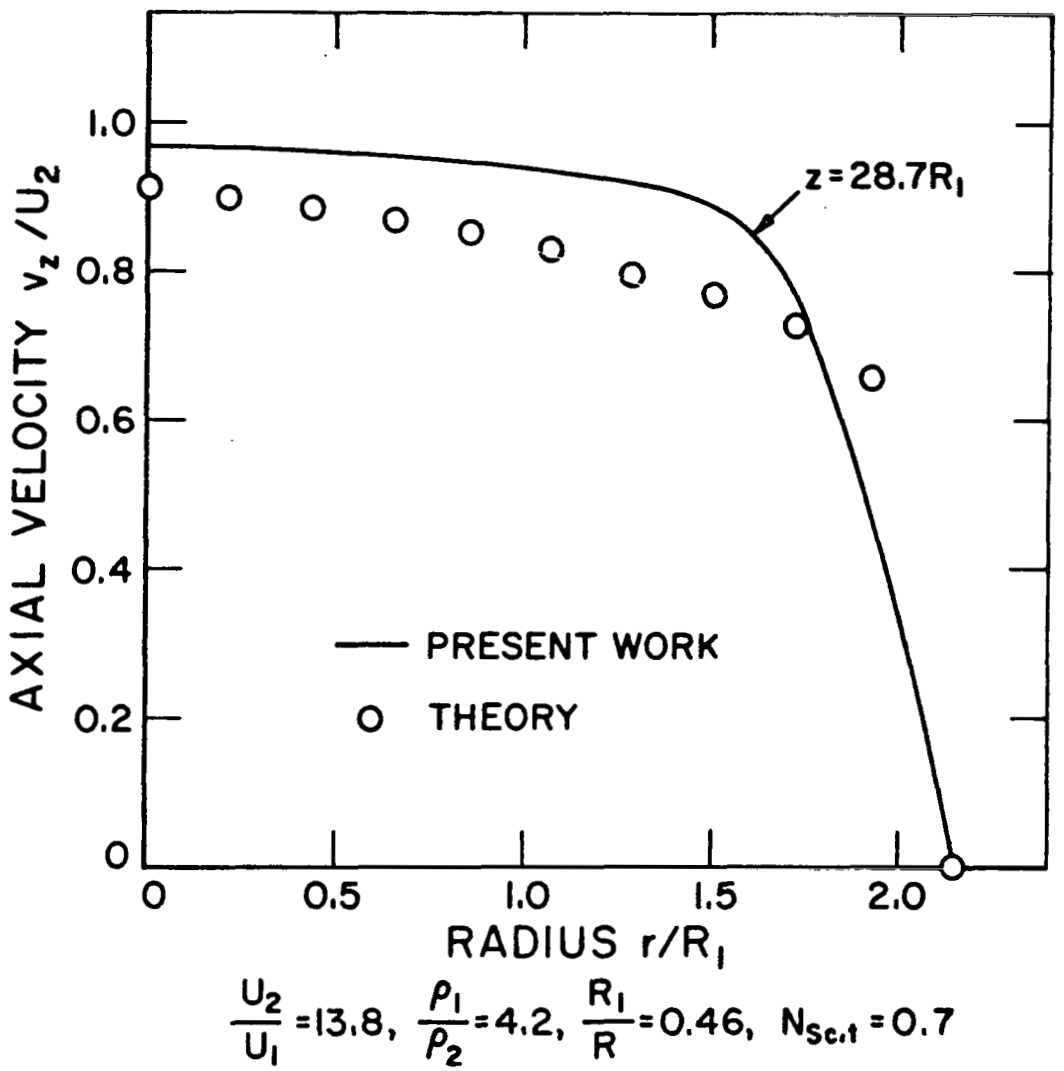

FIGURE 12 continued. FULLY DEVELOPED AXIAL VELOCITY PROFILES.

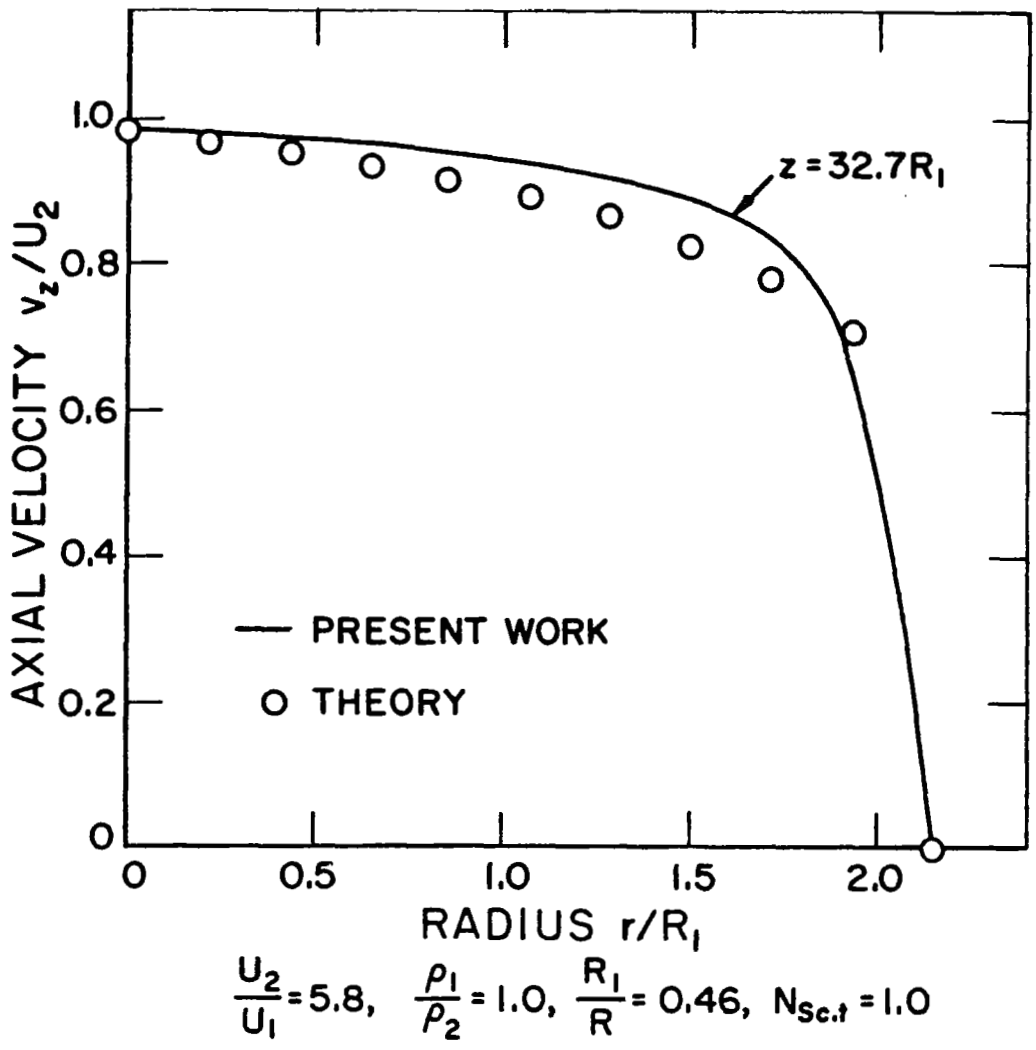

FIGURE 12 concluded. FULLY DEVELOPED AXIAL VELOCITY PROFILES.

CHAPTER 5

CONCLUSION

Turbulent heterogeneous mixing in the initial region of circular axisymmetric jets has been studied. An isothermal non-reacting binary system was considered and it consisted of a slow moving central jet of a heavy gas and a fast moving annular stream of a light gas. Such a system is characteristic of a gas core nuclear rocket. Therefore, the results obtained in the present investigation provide useful information about the flow phenomena occurring in a gaseous nuclear rocket.

The flow problem was formulated as a boundary value problem using the turbulent boundary layer equations. A phenomenological model was used for the turbulent kinematic eddy viscosity ϵ_v and the eddy diffusivity ϵ_m was obtained therefrom by considering the turbulent Schmidt number $N_{Sc,t}$ to be a parameter of the problem. The solution of the flow problem was obtained using an explicit finite difference scheme. The numerical stability of this scheme was ensured by satisfying Karplus' stability criterion.

The phenomenological model used for the eddy viscosity ϵ_v contains an empirical correlating parameter σ. For unconfined mixing of uniform density streams, the parameter σ has been shown to be constant throughout the flow field, with its value depending only on the entrance velocity ratio U_2/U_1 .[40] For the

present problem of confined heterogeneous mixing, the parameter σ was varied radially. While the shape of the radial profile of this parameter was arrived at by consideration of mixing as it occurs in the initial region of the flow field, its value was determined by correlation of the analytical results with available experimental data for the flow systems of present interest. Results were obtained for the four confined jet mixing configurations listed in Table I, Chapter 4, and are correlated with the corresponding experimental data of Reference 2. These correlations lead to the following conclusions.

As the velocity ratio U_2/U_1 increases, or the density ratio ρ_1/ρ_2 decreases, mixing becomes faster, thereby leading to the presence of positive axial pressure gradient dp/dz in the initial mixing region. The magnitude of the positive pressure gradient dp/dz increases with increase in the velocity ratio U_2/U_1 or decrease in the density ratio ρ_1/ρ_2.

For the range of parameters investigated, a possible formulation of the kinematic eddy viscosity coefficient ϵ_v is given by Equation (32), where the correlating parameter σ is the sum of a constant quantity and a radially varying quantity. As the velocity ratio U_2/U_1 increases, or the density ratio ρ_1/ρ_2 decreases, the radially varying part in the parameter σ diminishes and the constant part dominates. The use of such radial variation of the parameter σ and the satisfactory correlations thereby obtained, show that for confined heterogeneous

mixing, the kinematic eddy viscosity ϵ_v varies significantly in the transverse direction. Nevertheless, the dynamic eddy viscosity $\rho\epsilon_v$ does not exhibit strong radial variation. Similar observations have also been reported in References 33 and 47.

The turbulent Schmidt number $N_{Sc,t} = 0.7$ was used throughout the analysis (except for the homogeneous case, with $\rho_1 = \rho_2$, where $N_{Sc,t} = 1.0$). Results obtained with $N_{Sc,t} = 0.6$ and 0.8 showed that a small variation of the turbulent Schmidt number $N_{Sc,t}$ causes no significant changes in the velocity profiles, although the corresponding changes in the density near the jet axis are not negligible.

Finally, it must be mentioned that experimental data were available only for a limited number of jet mixing configurations with parameters having values within the range of present interest. For example, as seen in Table I, data were available for radius ratios $R_1/R = 0.46$ only. If the experimental data with different radius ratios were available, correlation with the analysis would enable the constant and the varying parameters comprising σ to be characterized in terms of some suitable grouping of the ratios U_2/U_1, ρ_1/ρ_2, and R_1/R. Additional experimental results are necessary in order to explore further the versatility of the analysis developed, as well as to substantiate the conclusions obtained in the present investigation.

REFERENCES

1. Ghia, Kirti N., Torda, T. Paul, and Lavan, Zalman, "Laminar Mixing of Heterogeneous Axisymmetric Coaxial Confined Jets", NASA-CR-72480, Nov. 1968.

2. Leithem, J., Kulik, R. A., and Weinstein, H., "Ducted Turbulent Mixing between Coaxial Streams," NASA CR-1335, 1969.

3. Craya, A., and Curtet, R., "On the Spreading of a Confined Jet" (in French). Comptes-rendus Academie des Sciences. Paris, vol. 241, pp. 621-622, 1955.

4. Curtet, R., "Confined Jets and Recirculation Phenomena with Cold Air," Combustion and Flame, London, Vol. 2, No. 4, December 1958.

5. Curtet, R., "On the Flow of an Enclosed Jet," (in French), Publication Scientifiques et Techniques du Ministere de l'Air, Paris, no. 359, 1960. Translation by U.S. Dept. of Commerce, Office of Technical Services, Joint Publications Research Service, "On Confined Jet Flow," DO-49-186-003-03535 JPRS; R-2934-D Jan. 4, 1963.

6. Curtet, R., and Ricou, F. P., "On the Tendency to Self-Preservation in Axisymmetric Ducted Jets," Journal of Basic Engineering, Transactions of ASME, December 1964.

7. Curtet, R., and Barchilon, M., "Some Details of the Structure of an Axisymmetric Confined Jet with Backflow," Journal of Basic Engineering, Transactions of ASME, December 1964.

8. Becker, H. A., Hottel, H. C., and Williams, G. C., "Mixing and Flow in Ducted Turbulent Jets," Ninth (International) Symposium on Combustion, Academic Press, New York, 1965.

9. Hill, P. G., "Turbulent Jets in Ducted Streams," Journal of Fluid Mechanics, Vol. 22, 1965.

10. Hill, P. G., "Incompressible Jet Mixing in Converging-Diverging Axisymmetric Ducts, " Journal of Basic Engineering, Transactions of ASME, 1966.

11. Exley, J. T., Flow Separation in Confined Jet Mixing, Master's Thesis, The Pennsylvania State University, 1969.

12. Dealy, J. M., "The Confined Circular Jet with Turbulent Source," Symposium on Fully Separated Flows, ASME, New York, November 1960.

13. Dealy, J. M., Momentum Exchange in a Confined Circular Jet with Turbulent Source, Ph.D. Thesis, University of Michigan, 1964.

14. Trapani, R. D., "An Experimental Study of Bounded and Confined Jets," Advances in Fluidics, ASME, pp. 1-13, 1967. Also, Fluidics Report 22, Harry Diamond Laboratories, November 1966.

15. Mikhail, S., "Mixing of Coaxial Streams Inside a Closed Conduit," Journal of Mechanical Engineering Science, Vol. 2, No. 1, pp. 59-68, March 1960.

16. Peters, C. E., Phares, W. J., and Cunningham, T. H. M., "Theoretical and Experimental Studies of Ducted Mixing and Burning of Coaxial Streams," Presented at AIAA 7th Aerospace Science Meeting, January 20-22, 1969. Paper No. 69-85.

17. Peters, C. E., "Turbulent Mixing and Burning of Coaxial Streams Inside a Duct of Arbitrary Shape," AEDC-TR-68-270, January 1969, (AD 680 397).

18. Peters, C. E., and Cunningham, T. H. M., "Further Experiments on Mixing of Bounded Coaxial Streams," AEDC-TR-68-136, October 1968, (AD 676 646).

19. Peters, C. E., and Wehofer, S., "Constant Area Mixing on Non-Isoenergetic Coaxial Compressible Streams," AEDC-TR-61-18, January 1962, (AD 270 156).

20. Emmons, D. L., "Analysis of the Turbulent Mixing between a Reactive Gas-Particle Rocket Exhaust and a Confined Airstream," AIAA Paper No. 65-609, June 1965. Also, Boeing Document D2-36251-1, February 1965.

21. Cohen, L. S., "An Analytical Study of the Mixing and Nonequilibrium Chemical Reaction of Ducted Compressible Streams," AIAA Paper 66-617, Second Propulsion Joint Specialist Conference, Colorado Springs, Colorado, June 13-17, 1966.

22. Edelman, R. and O. Fortune, "An Analysis of Mixing and Combustion in Ducted Flows," AIAA 6th Aerospace Science Meeting, New York, January, 1968, Paper 68-114.

23. Karplus, W. J., "An Electric Circuit Theory Approach to Finite Difference Stability," Transactions AIEE, Vol. 77, Part 1, 1958.

24. Libby, P. A., "Theoretical Analysis of Turbulent Mixing of Reactive Gases with Application to Supersonic Combustion of Hydrogen," ARS J. Vol. 32, pp. 388-396, March 1962.

25. Weinstein, H., and Todd, C. A., "Analysis of Mixing of Coaxial Streams of Dissimilar Fluids Including Energy-Generation Terms," NASA TN D-2123, March 1964.

26. Zakkay, V., and Krause, E., "Mixing Problems with Chemical Reactions," Supersonic Flow, Chemical Processes and Radiative Transfer, Pergamon Press, New York, 1964.

27. Taylor, G. I., "Statistical Theory of Turbulence," Proc. Roy. Society, A 151, 1935.

28. Schlichting, H., Boundary Layer Theory, McGraw-Hill Book Co., New York, 1964.

29. Pai, S. I., Fluid Dynamics of Jets, D. van Nostrand Company, Inc., 1954.

30. Hinze, J. O., Turbulence, McGraw-Hill Book Co., New York, 1959.

31. Schetz, J. A., "Analysis of the Mixing and Combustion of Gaseous and Particle-Laden Jets in an Air Stream," AIAA Paper No. 69-33, January 1969.

32. Forstall, W. Jr., and Shapiro, A. H., "Momentum and Mass Transfer in Coaxial Jets," J. Applied Mechanics, Vol. 7, No. 12, 1950.

33. Alpinieri, L. J., "Turbulent Mixing of Coaxial Jets," AIAA Journal Vol. 2, No. 9, 1964. Also, An Experimental Investigation of the Turbulent Mixing of Non-Homogeneous Coaxial Jets," PIBAL Report No. 789, August 1963.

34. Ferri, A., Libby, P. A., and Zakkay, J., "Theoretical and Experimental Investigation of Supersonic Combustion," Third Congress, International Council of the Aeronautical Sciences, Spartan Books, Baltimore, Md., 1964. Also, PIBAL Report No. 713, September 1962.

35. Ragsdale, R. G., and Edwards, O. J., "Turbulent Coaxial Mixing of Dissimilar Gases at Nearly Equal Stream Velocities," NASA TM X-52082, 1965.

36. Corrsin, S., and Uberoi, M. S., "Further Experiments on the Flow and Heat Transfer in a Heated Turbulent Air Jet," NACA Report 998, 1950.

37. Keagy, W. R., and Weller, A. E., "A Study of Freely Expanding Inhomogeneous Jets," Proc. Heat Transfer and Fluid Mechanics Institute, Amer. Soc. Mech. Engrs., New York, 1949.

38. Ting, L., and Libby, P. A., "Remarks on the Eddy Viscosity in Compressible Mixing Flows," J. Aerospace Sci., Vol. 27, No. 10, pp. 797-798, October 1960.

39. Bauer, P. T., Zumwalt, G. W., and Fila, L. H., "A Numerical Method and an Extention of the Korst Jet Mixing Theory for Multispecie Turbulent Jet Mixing," AIAA Paper No. 68-112, New York, January 1968. Also, An Eulerian Numerical Method for Multispecie, Turbulent Supersonic Jet Mixing, Ph.D. Thesis, Oklahoma State University, July 1968.

40. Korst, H. H., and Chow, W. L., "Non-Isoenergetic Turbulent (Pr_t = 1) Jet Mixing between Two Compressible Streams at Constant Pressure," NASA CR-419, April 1966.

41. Wood, B., Diffusion in a Laminar Confined Jet, D.Sc. Thesis, Massachusetts Institute of Technology, 1964.

42. Shavit, G., and Lavan, Z., Private Communications, Illinois Institute of Technology, Chicago, Illinois.

43. Weinstein, H., and Todd, C. A., "A Numerical Solution of the Problem of Mixing of Laminar Coaxial Streams of Greatly Different Densities - Isothermal Cases," NASA TN D-1534, 1963.

44. Donaldson, C. duP., and Gray, K. E., "Theoretical and Experimental Investigation of the Compressible Free Mixing of Two Dissimilar Gases," AIAA Journal, Vol. 4, No. 11, November 1966.

45. Boehman, L. I., "Mass and Momentum Transport Properties in Isoenergetic Coaxial Flows," Ph.D. Thesis, Illinois Institute of Technology, 1967. Also, "Research on Mixing of Coaxial Streams," ARL 67-0058, March 1967.

46. Baker, R. L., and Weinstein, H., "Experimental Investigation of the Mixing of Two Parallel Streams of Dissimilar Fluids," NASA CR-956.

47. Zakkay, V., and Krause, E., "The Radial Variation of the Eddy Viscosity in Compressible Turbulent Jet Flows," International Journal of Heat Mass Transfer, Vol. 8, pp.1047-1050, Pergamon Press, 1965.

NASA-Langley, 1970 — 12 E-5544